UNIVERSITY OF THESSALY

SCHOOL OF ENGINEERING

DEPARTMENT OF MECHANICAL ENGINEERING

DIPLOMA THESIS

CONSTITUTIVE MODELING AND NUMERICAL METHODS FOR TRIP STEELS

by

GKARSEN DAGKLIS ANGELOS

Submitted for the partial fulfilment of the requirements for the diploma of Mechanical Engineer.

Volos, 2019

Approved by the members of the Committee:

First Member	*Professor Nikolaos Aravas*
(Supervisor)	*Department of Mechanical Engineering, University of Thessaly*
Second Member	*Assistant Professor Alexis Kermanidis*
	Department of Mechanical Engineering, University of Thessaly
Third Member	*Assistant Professor Michalis Agoras*
	Department of Mechanical Engineering, University of Thessaly

Contents

List of Figures

List of Tables

0.1 Acknowledgements

First of all, I would like to express my gratitudes to my supervising professor, Dr. Nikolaos Aravas for his assistance and guidance during the creation of my diploma thesis. I would like to thank the other members of my thesis committee, Dr M. Agoras and Dr A. Kermanidis for their valuable comments . Also, I want to graditute Dr. Ioanna Papadioti for her advice and help. Finally, I am grateful to my family, my parents and my sister, for their unconditional love and support in every aspect of my life.

Chapter 1

Introduction

1.1 Scope of the present work

The scope of the present work is to develop a constitutive model for the mechanical behaviour of TRIP (Transformation Induced Plasticity) steels. TRIP steels are basically composite materials with evolving volume fractions of the constituent phases. Specifically we consider three-phase TRIP steels that consist of a ferritic matrix with dispersed austenite, which transforms gradually into martensite as the material deforms plastically. The constitutive model is used for the calculation of "forming limit diagrams" for sheets made of TRIP steels. Calculations are also conducted for a non-transforming steel for comparison purposes.

It is well known that the microstructure and the properties of a steel are determined by the chemical composition and the thermal processing. TRIP steels is a category of steels, where, plastic deformation results in the transformation of the austenitic phase into martensite. Previous works on TRIP steels, such as the work of Papadioti [12] and Papatriantafillou [13], have shown that TRIP phenomena affect the mechanical response of the material, and thus, they have to be considered in the development of the constitutive models.

Difficulties in the development of a model like this arise from two main factors. The first is the fact that TRIP steels are composite materials and the second is the constant evolution of the volume fractions of the constituent phases due to the plastic-induced martensitic transformation.

In the works referred previously, the model of Olson and Cohen [7] has been used to describe the kinetics of the evolution of martensite volume fraction. In this thesis, we use the model developed by Haidemenopoulos et. al [5]. This model predicts the evolution of martensite during strain-induced transformation taking into account the effects of the chemical composition of austenite, temperature, average size of austenite particles and stress triaxiality.

The constitutive equations are developed by using the non-linear homogenization methods developed by Ponte Castañeda and co-workers ([15],[17],[18]). The crucial advantage of the aforementioned non-linear homogenization methods lies in the fact that besides their ability to deliver accurate estimates for the macroscopic behavior of nonlinear composites, they also provide additional information about the average stress and strain fields in each of the individual phases. The knowledge of these fields, in turn, allows the estimation of

the evolution of microstructure at finite deformations, which leads to anisotropic hardening or softening of the composite material and finally to failure ([2],[3],[4],[6],[22]). A very interesting application of these non-linear homogenization theories was presented recently by Papadioti, Danas, Aravas [11], who developed a methodology for the analytical estimation of the effective yield function of isotropic composites; this methodology is used in the current work to define the plastic behavior and the microstructure evolution in TRIP steels.

1.2 TRIP steels

As the name TRIP (Transformation Induced Plasticity) implies, plastic deformation denotes martensitic transformation of retained austenite. Martensitic transformation results in a different hardening curve, with a greater strain until failure. This change results in higher ductility, fracture toughness and formability for this material.

There are two types of TRIP steels, the austenitic TRIP steels and multiphase low-alloy TRIP steels. The second type is a composite material, consisting of multiple phases as ferrite, retained austenite, martensite and bainite. They are typically used in the automotive industry, in applications where high formability is required.

In this thesis, we are dealing with a low-alloy Transformation-Induced Plasticity steels consisting of ferrite, retained austenite with a volume fraction of $10-15\%$, which transforms gradually into martensite as the material deforms plastically. The microstructure of the material consists of a ferritic matrix with randomly distributed spherical inclusions of the other phases.

An important aspect of the martensitic transformation is the strain softening which occurs due to the strain associated with the transformation process. This strain softening is accounted for by introducing in the constitutive model an additional deformation rate that is proportional to the rate of increase of the volume fraction of martensite. The total deformation rate can be split into elastic, plastic and transformation parts. Standard isotropic linear hypoelasticity of homogeneous solids is used in order to describe the elastic behavior of the TRIP steels since the elastic properties of all phases are fundamentally the same. The constitutive equation of the plastic part is determined by using the homogenization theory. The transformation part has both deviatoric and volumetric parts and is proportional to the rate of change of the volume fraction of martensite due to martensitic transformation, which is described by the transformation kinetics model proposed by Haidemenopoulos et al [5]. This model describes the fraction of the martensite formed as a function of the plastic strain, where the austenite is present in the form of dispersed particles. The model also predicts the effects of austenite particle size, the chemical composition of the austenite, temperature and the stress triaxiality.

1.3 The Homogenization method

The homogenization method is used to estimate the macroscopic response and the average response of the phases of a composite material with N-phases. This work uses the non-linear

variational homogenization method (Ponte Castañeda, [15]), or the modified secant method (Suquet, [20]), which makes use of a linear comparison composite (LCC) material, to estimate the effective response of an N-phase non-linear composite material. This approach leads to an optimization problem, for N-1 variables, which has to be solved numerically, except of the 2-phase case. A very interesting application of these non-linear homogenization theories was presented recently by Papadioti, Danas, Aravas [11].

At this point, we will present a brief description of this method. First of all, we consider that all the phases are incompressible and viscoplastic. Each phase is characterized by a power law stress potential of the form:

$$U^{(r)}\left(\sigma_e^{(r)}\right) = \frac{\sigma_0^{(r)}\dot{\varepsilon}_0}{n^{(r)}+1}\left(\frac{\sigma_e^{(r)}}{\sigma_0^{(r)}}\right)^{n^{(r)}+1}, \tag{1.1}$$

where $\sigma_0^{(r)}$, $\dot{\varepsilon}_0$ and $n^{(r)}$ are constants.

The macroscopic behaviour of the composite material is determined as:

$$\mathbf{D} = \mathbf{D}(\boldsymbol{\sigma}) = \frac{\partial \tilde{U}}{\partial \boldsymbol{\sigma}}, \tag{1.2}$$

where $\boldsymbol{\sigma}$ and $\mathbf{D}$ are the macroscopic stress and deformation rate of the composite material, while $\tilde{U} = \tilde{U}(\boldsymbol{\sigma})$ is the effective viscoplastic stress potential.

For the estimation of $\tilde{U}$ the following form has been proposed by Ponte Castañeda [16]:

$$\tilde{U} = \sup_{\mu^{(r)}\geq 0}\left[\tilde{U}_L\left(\sigma_e, \tilde{\mu}\left(\mu^{(r)}\right)\right) - \sum_{r=1}^{N} c^{(r)} v^{(r)}\left(\mu^{(r)}\right)\right], \tag{1.3}$$

$$\tilde{U}_L = \frac{\sigma_e^2}{6\tilde{\mu}\left(\mu^{(r)}\right)}, \tag{1.4}$$

$$v^{(r)}\left(\mu^{(r)}\right) = \sup_{\sigma_e^{(r)}\geq 0}\left[U_L^{(r)}\left(\sigma_e^{(r)}, \mu^{(r)}\right) - U^{(r)}\left(\sigma_e^{(r)}\right)\right], \tag{1.5}$$

$$U_L^{(r)} = \frac{{\sigma_e^{(r)}}^2}{6\mu^{(r)}} \tag{1.6}$$

and

$$\tilde{\mu}\left(\mu^{(r)}\right) = \left(\sum_{s=1}^{N}\frac{c^{(s)}\mu^{(s)}}{3\mu_0+2\mu^{(s)}}\right)\left(\sum_{r=1}^{N}\frac{c^{(r)}}{3\mu_0+2\mu^{(r)}}\right)^{-1}, \tag{1.7}$$

where μ_0 is a "reference viscosity" to be chosen appropriately.

Also, it is proven that the average deformation rate field in the phases $\mathbf{D}^{(r)}$, for an isotropic matrix and a uniform distribution of spherical inclusions, takes the form:

$$\mathbf{D}^{(r)} = a^{(r)}\mathbf{D}, \tag{1.8}$$

$$a^{(r)} = \frac{1}{3\mu_0+2\hat{\mu}^{(r)}}\left(\sum_{s=1}^{N}\frac{c^{(s)}}{3\mu_0+2\hat{\mu}^{(s)}}\right)^{-1} \tag{1.9}$$

where $\hat{\mu}^{(r)}$ are the optimal values of $\mu^{(r)}$ derived from the optimisation problem (1.3).

We set all the creep exponents of the phases equal ($n^{(1)} = n^{(2)} = \cdots = n^{(N)} = n$) and then assume that all the phases are perfectly plastic ($n \to \infty$), so, we prove that the macroscopic response of composite material is also perfectly plastic. In addition, the yield stress of the composite material is given by the following expression:

$$\tilde{\sigma}_0\left(c^{(i)}, \sigma_0^{(i)}\right) = \sqrt{\inf_{\substack{y^{(1)}=1 \\ y^{(i)}\geq 0,\, i=2,3}} \left(\sum_{r=1}^{3} c^{(r)} {\sigma_0^{(r)}}^2 y^{(r)}\right)\left(\sum_{p=1}^{3} \frac{c^{(p)}}{3y^{(p)} + 2y_0}\right)\left(\sum_{(s=1)}^{3} \frac{c^{(s)} y^{(s)}}{3y^{(s)} + 2y_0}\right)^{-1}}, \tag{1.10}$$

where $y^{(r)} = \dfrac{\mu^{(1)}}{\mu^{(r)}}$ and $y_0 = \dfrac{\mu^{(1)}}{\mu_0}$.

In this case, we have a 3-phase material, so we have to solve an optimization problem of two variables, numerically. For this purpose, CONMAX software will be used. The composite is assumed to behave as "incrementally perfectly plastic" with a flow stress $\tilde{\sigma}_0$, which is updated at every increment. The value of $\tilde{\sigma}_0$ is calculated by the solution of the corresponding optimization problem (1.10) using the values $\sigma_0^{(i)}$ at each increment. The solution of the optimization problem (1.10) defines also the optimal values $\hat{y}^{(i)}$, which determine the corresponding strain concentration factors in (1.9) for the increment.

1.4 Thesis overview

In Chapter 2, we develop the constitutive model for three-phase TRIP steels. The homogenization techniques for non-linear composites, described in Chapter 1, are used to determine the effective properties and overall behavior of TRIP steels. Standard isotropic linear hypoelasticity of homogeneous solids is used in order to describe the elastic behavior of the TRIP steels and the martensitic transformation is described by the transformation kinetics model proposed by Haidemenopoulos et al [5].

In Chapter 3, we develop a methodology for the numerical integration of the resulting elastoplastic constitutive equations and the model is implemented into the ABAQUS [1]. We also provide an expression for the Linearization moduli, which is required in a finite element analysis.

In Chapter 4, we develop a method for the numerical integration of the constitutive model under plane stress conditions. In these problems the out-of-plane component of the deformation gradient is not defined kinematically and the general method needs to be modified.

Chapter 5 is concerned with the calculation of the Forming Limit Diagrams for sheets made of TRIP steels. Calculations are also conducted for a non-transforming steel for comparison purposes.

Finally, Chapter 6 provides a brief summary of the contribution of this work together with some prospects for future work.

1.5 Notations

In this thesis, all tensors will be indicated by bold letters. Every component of a tensor will be written with respect to a coordinate system with base vectors $\mathbf{e}_i$ for $i = 1, 2, 3$. The sum convention will be used also, for repeated indices in the same term. If $\mathbf{a}$ and $\mathbf{b}$ are vectors, $\mathbf{A}$ and $\mathbf{B}$ are second order tensors and $\boldsymbol{\mathcal{K}}$ and $\boldsymbol{\mathcal{M}}$, then the following products are defined:
$\mathbf{a} \cdot \mathbf{b} = a_i b_i$,
$\mathbf{A} : \mathbf{B} = A_{ij} B_{ij}$,
$(\mathbf{ab})_{ij} = a_i b_j$,
$(\mathbf{A} \cdot \mathbf{B})_{ij} = A_{ik} B_{kj}$,
$(\boldsymbol{\mathcal{K}} : \mathbf{A})_{ij} = \mathcal{K}_{ijkl} A_{kl}$,
$(\boldsymbol{\mathcal{K}} : \boldsymbol{\mathcal{M}})_{ijkl} = \mathcal{K}_{ijpq} \mathcal{M}_{pqkl}$.

We will use the Lagrangian description of motion. In the undeformed configuration, or at time $t = 0$, the position of any material point is denoted by $\mathbf{X}$. At any deformed configuration, at time t, the position of the material point that where on $\mathbf{X}$ at $t = 0$, is represented by $\mathbf{x} = \mathbf{x}(\mathbf{X}, t)$, where $\mathbf{X}$ and t are the independent variables.

For this description we will use the following definitions:
The deformation gradient: $\mathbf{F}(\mathbf{X}, t) = \frac{\partial \mathbf{x}}{\partial \mathbf{X}}$,
The velocity of a particle: $\mathbf{u}(\mathbf{X}, t) = \frac{\partial \mathbf{x}}{\partial t}$,
The velocity gradient: $\mathbf{L}(\mathbf{x}, t) = \frac{\partial \mathbf{u}}{\partial \mathbf{x}}$.

Chapter 2

Constitutive Modeling of TRIP steels

In this chapter we present the constitutive equations which describe the mechanical behaviour of a three-phase low-alloy TRIP steel, consisting of ferrite, austenite and martensite. The following labels are used for the constituent phases: (1) for ferrite, (2) or (a) for austenite and (3) or (m) for martensite. The constitutive equations are developed for the case of finite geometry changes.

2.1 Constitutive formulation

As we have already mentioned, an important aspect of the martensitic transformation is the strain softening which occurs due to the strain associated with the transformation process. This strain softening is accounted for by introducing in the constitutive model an additional deformation rate that is proportional to the rate of increase of the volume fraction of martensite. The total deformation rate can be split into elastic, plastic and transformation parts:

$$\mathbf{D} = \mathbf{D}^e + \mathbf{D}^p + \mathbf{D}^{TRIP} \tag{2.1}$$

2.1.1 The elastic part

Standard isotropic linear hypoelasticity of homogeneous solids is used in order to describe the elastic behavior of the TRIP steels since the elastic properties of all phases are fundamentally the same. The constitutive equation for $\mathbf{D^e}$ is written as

$$\overset{\triangledown}{\boldsymbol{\sigma}} = \boldsymbol{\mathcal{L}}^e : \mathbf{D}^e \tag{2.2}$$

or

$$\mathbf{D}^e = \boldsymbol{\mathcal{M}}^e : \overset{\triangledown}{\boldsymbol{\sigma}} \tag{2.3}$$

where $\overset{\triangledown}{\boldsymbol{\sigma}} = \dot{\boldsymbol{\sigma}} - \mathbf{W} \cdot \boldsymbol{\sigma} + \boldsymbol{\sigma} \cdot \mathbf{W}$ is the Jaumann derivative of the stress tensor and $\mathbf{W} = \frac{1}{2}\left(\mathbf{L} - \mathbf{L}^T\right)$ is the antisymmetric part of the velocity gradient $\mathbf{L}$.
$\boldsymbol{\mathcal{L}}^e$ and $\boldsymbol{\mathcal{M}}^e$ are the elastic and elastic compliance tensors respectively:

$$\boldsymbol{\mathcal{L}}^e = 2\mu\boldsymbol{\mathcal{K}} + 3\kappa\boldsymbol{\mathcal{J}}$$

and

$$\boldsymbol{\mathcal{M}}^e = \boldsymbol{\mathcal{L}}^{e-1} = \frac{1}{2\mu}\boldsymbol{\mathcal{K}} + \frac{1}{3\kappa}\boldsymbol{\mathcal{J}}$$

μ and κ are the elastic constants of steel. $\boldsymbol{\mathcal{K}}$ and $\boldsymbol{\mathcal{J}}$ are the deviatoric and the spherical part of the fourth-order identity tensor $\mathcal{I}_{ijkl} = \frac{1}{2}\left(\delta_{ik}\delta_{jl} + \delta_{il}\delta_{jk}\right)$, so:

$$\boldsymbol{\mathcal{J}} = \frac{1}{3}\boldsymbol{\delta}\boldsymbol{\delta}$$

and

$$\boldsymbol{\mathcal{K}} = \boldsymbol{\mathcal{I}} + \boldsymbol{\mathcal{J}}$$

2.1.2 The plastic part

The plastic part $\mathbf{D}^p$ of the deformation rate is determined in terms of the plastic properties of the constituent phases by using the homogenization theory described in Chapter 1. As it is mentioned in [11], the flow rule can be written as:

$$\mathbf{D}^p = \frac{\partial \tilde{U}}{\partial \boldsymbol{\sigma}} = \dot{\bar{\varepsilon}}\mathbf{N}, \quad \mathbf{N} \equiv \frac{3}{2\sigma_e}\mathbf{s}, \tag{2.4}$$

where $\mathbf{s}$ is the deviatoric part of the Cauchy stress tensor $\boldsymbol{\sigma}$. The rate of the equivalent plastic strain $\dot{\bar{\varepsilon}}$ is by definition $\dot{\bar{\varepsilon}} = \sqrt{\frac{2}{3}\mathbf{D}^p : \mathbf{D}^p}$. The following relation for the rate of the equivalent plastic strain can be proved:

$$\dot{\bar{\varepsilon}} = \frac{\sigma_e}{3\tilde{\mu}}, \tag{2.5}$$

where $\sigma_e = \sqrt{\frac{3}{2}\mathbf{s} : \mathbf{s}}$ is the von Mises equivalent stress and $\tilde{\mu} = \tilde{\mu}\left(c^{(r)}, \sigma^{(r)}_{(0)}(\bar{\varepsilon}^{(r)})\right)$ is obtained through Homogenization theory.
Also, we can find the plastic deformation for each phase:

$$\mathbf{D}^{p(i)} = \alpha^{(i)}\mathbf{D}^p \tag{2.6}$$

where $\alpha^{(i)} = \alpha^{(i)}\left(c^{(r)}, \sigma^{(r)}_{(0)}(\bar{\varepsilon}^{(r)})\right)$ are also determined by Homogenization theory. Finally we can derive the following relation between the average rate of the equivalent strain of each phase and the rate of the equivalent plastic strain of the material:

$$\dot{\bar{\varepsilon}}^{(i)} = \sqrt{\frac{2}{3}\mathbf{D}^{p(i)} : \mathbf{D}^{p(i)}} = a^{(i)}\dot{\bar{\varepsilon}} \tag{2.7}$$

More details about this formulation of the plastic part can be found in Papadioti [12].

2.1.3 The Transformation Part

The transformation part is inelastic and has both a deviatoric and a spherical part. For this part, Stringfellow [19] proposed the following form:

$$\mathbf{D}^{TRIP} = A(\sigma_e)\dot{f}\mathbf{N} + \frac{1}{3}\dot{\varepsilon}_v^p\boldsymbol{\delta} \tag{2.8}$$

where $A(\sigma_e)$ is a function of von Mises equivalent stress, f is the volume fraction of martensite, $\mathbf{N}$ is a second order tensor derived from the deviatoric part of the stress tensor, which has been already defined in (2.4), $\boldsymbol{\delta}$ is the second-order identity tensor and $\dot{\varepsilon}_v^p$ is the transformation dilatation rate and $A(\sigma_e)$ is a dimensionless quantity:

$$\dot{\varepsilon}_v^p = \Delta_v\dot{f}, \tag{2.9}$$

$$A(\sigma_e) = A_0 + A_1\frac{\sigma_e}{s_a^*} \tag{2.10}$$

where Δ_v is the relative volume change caused by martensetic transformation, A_0 and A_1 are dimensionless constants ans s_a^* is a reference austenite stress.

2.1.4 The evolution of the Martensitic phase

Haidemenopoulos et al [5] developed a model that describes the kinetics of the evolution of martensite volume fraction during the strain-induced transformation of dispersed austenite in low-alloy TRIP steels. The model is based on the Olson–Cohen theory of heterogeneous martensitic nucleation ([8],[9],[10]).

Martensitic transformation is dominated by two different mechanisms, the stress assisted and the strain inducted nucleation. In the first mechanism, martensite nucleates on pre-existing nucleation sites. In the second mechanism, new nucleation sites are created due to the plastic deformation of the austenite.

The model presented below predicts the evolution of martensite during strain-induced transformation taking into account the effects of the chemical composition of austenite, temperature, average size of austenite particles and stress triaxiality. The evolution equation for the volume fraction of martensite f derived by Haidemenopoulos et al [5] is of the form:

$$\dot{f} = \dot{c}^{(3)} = c^{(2)}A_f\dot{\bar{\varepsilon}}^{(2)} \tag{2.11}$$

where $c^{(2)}$ and $\dot{\bar{\varepsilon}}^{(2)}$ are the volume fraction and the equivalent plastic strain of the austenitic phase. A_f is a function of the equivalent plastic strain of the austenite and the stress triaxiality defined as :

$$A_f = A_f(\bar{\varepsilon}^{(2)}, \Sigma) = v_p km\left[N - N_v^{\varepsilon 0}\left(\bar{\varepsilon}^{(2)}\right)\right]\left(\bar{\varepsilon}^{(2)}\right)^{m-1}\exp\left(-a_\varepsilon n^*\right) \tag{2.12}$$

where v_p is the average volume of austenite particles, a_ε is a shape factor of strain-modified potency distribution, N is the maximum number of nucleation sites per unit austenite volume and $N_v^{\varepsilon 0}$ is the number of additional sites produced from plastic stain. k and m are also

constants. N and $N_v^{\varepsilon 0}$ are dimensionless quantities. N is given as a constant and $N_v^{\varepsilon 0}$ is a function of $\bar{\varepsilon}^{(2)}$:

$$N_v^{\varepsilon 0}\left(\bar{\varepsilon}^{(2)}\right) = N\left[1 - \exp\left(-k\left(\bar{\varepsilon}^{(2)}\right)^m\right)\right] \tag{2.13}$$

It should be noted that n^* is temperature-dependent through the chemical driving force ΔG_{ch} and stress-dependent through the mechanical driving force ΔG_σ. The critical value of n also depends on the chemical composition of the austenite through the compositional dependence of ΔG_{ch} and the frictional work of interface motion W_f [5]:

$$n^*(\sigma_e) = -\frac{2\gamma_s}{\rho}\frac{1}{\Delta G_{ch} + \Delta G_\sigma(\sigma_e) + E_{str} + W_f} \tag{2.14}$$

where γ_s is the fault interfacial energy (J/m^2), ρ is the density of atoms in fault plane (mol/m^2) and ΔG_{ch} ΔG_σ, E_{str}, W_f are the chemical driving force for martensitic transformation, the mechanical contribution to driving force, the elastic strain energy and the frictional work of interface motion, respectively. E_{str}, W_f and ΔG_{ch} are constants, while ΔG_{ch} is a function of equivalent stress σ_e and stress triaxiality Σ, given by:

$$\Delta G_\sigma(\sigma_e, \Sigma) = \sigma_e \frac{\partial \Delta G}{\partial \sigma_e}(\Sigma) \tag{2.15}$$

where

$$\frac{\partial \Delta G}{\partial \sigma_e}(\Sigma) = -0.715 - 0.3206\Sigma \qquad (J/mol \cdot MPa) \tag{2.16}$$

The following relations for ΔG_{ch} and W_f are proposed in the model:

$$W_f = 1.893 \times 10^3 {X_{Mn}}^{2/3} + 1.310 \times 10^4 {X_C}^{2/3}, \tag{2.17}$$

for Fe-C-Mn alloys, and

$$\Delta G_{chemical} = \Delta G_{chemical}(T)(J/mol). \tag{2.18}$$

where $\Delta G_{chemical}(T)$ is a linear function and it depends on the chemical composition of the alloy.

In the following the evolution equations for $c^{(1)}$ and $c^{(2)}$ are presented. Starting with the definition of the volume fraction:

$$c^{(i)} = \frac{V^{(i)}}{V} \tag{2.19}$$

we derive $\dot{c}^{(1)} = -c^{(1)}\dot{V}\big/V$. As we have mentioned previously, the martensitic transformation results in volumetric inelastic deformation. This phenomenon is described by the following relation:

$$\dot{\varepsilon}_v^p = \frac{\dot{V}}{V} \simeq \Delta_v \dot{f}, \tag{2.20}$$

where Δ_v is a constant. As a result the evolution rate of ferritic phase is related with $\dot{f}$ as:

$$\dot{c}^{(1)} = -c^{(1)}\frac{\dot{V}}{V} = -c^{(1)}\Delta_v \dot{f}. \tag{2.21}$$

and since $c^{(1)} + c^{(2)} + f = 1$ we find :

$$\dot{c}^{(2)} = -\left(\dot{c}^{(1)} + \dot{f}\right). \tag{2.22}$$

2.1.5 Summary of the constitutive equations

In this chapter we developed the constitutive equations for a 3-phase TRIP steel. These equations can be summarized as:

$$\mathbf{D} = \mathbf{D}^e + \mathbf{D}^p + \mathbf{D}^{TRIP}, \tag{2.23}$$

$$\overset{\triangledown}{\boldsymbol{\sigma}} = \boldsymbol{\mathcal{L}}^e : \mathbf{D}^e, \tag{2.24}$$

$$\mathbf{D}^p = \dot{\bar{\varepsilon}}\mathbf{N}, \quad \dot{\bar{\varepsilon}} = \frac{\sigma_e}{3\tilde{\mu}}, \tag{2.25}$$

$$\mathbf{D}^{TRIP} = A\left(\sigma_e\right)\dot{f}\mathbf{N} + \frac{1}{3}\dot{\varepsilon}_v^p\boldsymbol{\delta}, \tag{2.26}$$

where:

$$\mathbf{N} = \frac{3}{2\sigma_e}\mathbf{s}, \quad \sigma_e = \sqrt{\frac{3}{2}\mathbf{s} : \mathbf{s}}, \quad \dot{\varepsilon}_v^p = \Delta_v \dot{f}. \tag{2.27}$$

and the evolution equations of the volume fractions are given by:

$$\dot{c}^{(1)} = \Delta_v \dot{f}, \tag{2.28}$$

$$\dot{c}^{(3)} = \dot{f} = c^{(2)} A_f \dot{\bar{\varepsilon}}^{(2)}, \tag{2.29}$$

$$\dot{c}^{(2)} = -\left(\dot{c}^{(1)} + \dot{f}\right), \tag{2.30}$$

where

$$A_f = A_f\left(\bar{\varepsilon}^{(2)}, \Sigma\right). \tag{2.31}$$

2.2 Numerical Integration

In this section, we present a method for the numerical integration of the resulting constitutive equations of TRIP steels in the context of a displacement driven finite element formulation. In a finite element analysis, the solution of the problem is developed incrementally. We consider t as a time-like loading parameter, where t_n corresponds to the start of the increment and t_{n+1} to the end. Also, we assume that $\Delta t = t_{n+1}$–t_n is small. For any quantity $A(t)$, we use the notation $A\left(t_n\right) = A_n$ and $A\left(t_{n+1}\right) = A_{n+1}$ to represent the value of this quantity at the start and at the end of the increment, respectively. Finally, we set $\Delta A = A_{n+1} - A_n$. During an increment, or for $t_n < t < t_{n+1}$, we assume that the material is perfectly plastic in order to use the homogenization theory.

At the beginning of an increment, all the quantities needed to define the solution $\left(\mathbf{F}_n, \boldsymbol{\sigma}_n, c_n^{(r)}, \bar{\varepsilon}_n^{(i)}\right)$, are considered as known. In addition, as we are dealing with displacement driven analysis, the deformation gradient in the end of the increment, $\mathbf{F}_{n+1}$, is also given and the problem is to define $\left(\boldsymbol{\sigma}_{n+1}, c_{n+1}^{(r)}, \bar{\varepsilon}_{n+1}^{(i)}\right)$ at the end of each increment.

The time variation of the deformation gradient $\mathbf{F}$ during the time increment $[t_n, t_{n+1}]$ can be written as:

$$\mathbf{F}(t) = \Delta\mathbf{F}(t) \cdot \mathbf{F}_n = \mathbf{R}(t) \cdot \mathbf{U}(t) \cdot \mathbf{F}_n \tag{2.32}$$

where $\mathbf{R}(t)$ and $\mathbf{U}(t)$ are the rotation and right stretch tensors derived from Polar Decomposition of $\Delta\mathbf{F}(t)$.

The deformation gradient tensor $\mathbf{L} = \partial\mathbf{u}/\partial\mathbf{x}$ is written in terms of $\mathbf{F}(t)$ as:

$$\mathbf{L}(t) = \Delta\dot{\mathbf{F}}(t) \cdot \Delta\mathbf{F}^{-1}(t). \tag{2.33}$$

The deformation rate $\mathbf{D}(t)$ and spin $\mathbf{W}(t)$ tensors are the symmetric and anti-symmetric parts of $\mathbf{L}(t)$, so they are expressed as:

$$\mathbf{D}(t) = \frac{1}{2}\left(\mathbf{L}(t) + \mathbf{L}^T(t)\right) = \left[\Delta\dot{\mathbf{F}}(t) \cdot \Delta\mathbf{F}^{-1}(t)\right]_s, \tag{2.34}$$

$$\mathbf{W}(t) = \frac{1}{2}\left(\mathbf{L}(t) - \mathbf{L}^T(t)\right) = \left[\Delta\dot{\mathbf{F}}(t) \cdot \Delta\mathbf{F}^{-1}(t)\right]_a. \tag{2.35}$$

We assume that the eigenvectors of $\mathbf{U}(t)$ remain constant during the increment thus:

$$\mathbf{D}(t) = \mathbf{R}(t) \cdot \dot{\mathbf{E}}(t) \cdot \mathbf{R}^T(t), \tag{2.36}$$

$$\mathbf{W}(t) = \dot{\mathbf{R}}(t) \cdot \mathbf{R}^T(t) \tag{2.37}$$

and

$$\overset{\triangledown}{\boldsymbol{\sigma}}(t) = \mathbf{R}(t) \cdot \dot{\hat{\boldsymbol{\sigma}}} \cdot \mathbf{R}^T(t), \tag{2.38}$$

where $\mathbf{E}(t)$ is the logarithmic strain tensor and:

$$\hat{\boldsymbol{\sigma}}(t) = \mathbf{R}^T \cdot \boldsymbol{\sigma}(t) \cdot \mathbf{R}. \tag{2.39}$$

We should mention that at the start of the increment, or at $t = t_n$:

$$\mathbf{R}_n = \mathbf{U}_n = \boldsymbol{\delta}, \quad \mathbf{E}_n = \mathbf{0}, \quad \hat{\boldsymbol{\sigma}}_n = \boldsymbol{\sigma}_n \tag{2.40}$$

whereas at the end of the increment $t = t_{n+1}$:

$$\Delta\mathbf{F}_{n+1} = \mathbf{F}_{n+1} \cdot {\mathbf{F}_n}^{-1} = \mathbf{R}_{n+1} \cdot \mathbf{U}_{n+1} = known, \tag{2.41}$$

and

$$\mathbf{E}_{n+1} = \ln \mathbf{U}_{n+1} = known. \tag{2.42}$$

Therefore, the constitutive equations (2.1), (2.2), (2.4), and (2.8) can be written in the following form:

$$\mathbf{D} = \mathbf{D}^e + \mathbf{D}^p + \mathbf{D}^{TRIP} \quad \Rightarrow \quad \dot{\mathbf{E}} = \dot{\mathbf{E}}^e + \dot{\mathbf{E}}^{in} \tag{2.43}$$

$$\overset{\triangledown}{\boldsymbol{\sigma}} = \boldsymbol{\mathcal{L}}^e : \mathbf{D}^e \quad \Rightarrow \quad \dot{\hat{\boldsymbol{\sigma}}} = \boldsymbol{\mathcal{L}}^e : \dot{\mathbf{E}}^e \tag{2.44}$$

$$\left.\begin{array}{r} \mathbf{D}^p = \dot{\bar{\varepsilon}}\mathbf{N} \\ \mathbf{D}^{TRIP} = A(\sigma_e)\dot{f}\mathbf{N} + \frac{1}{3}\dot{\varepsilon}_v^p\boldsymbol{\delta} \end{array}\right\} \quad \Rightarrow \quad \dot{\mathbf{E}}^{in} = \left(\dot{\bar{\varepsilon}} + A(\sigma_e)\dot{f}\right)\hat{\mathbf{N}} + \frac{1}{3}\dot{\varepsilon}_v^p\boldsymbol{\delta} \tag{2.45}$$

From equation (2.6) and the definition of the equivalent plastic stain $\dot{\bar{\varepsilon}} = \sqrt{\frac{3}{2}\mathbf{D}^p : \mathbf{D}^p}$, we can derive the following relation between the rate of the macroscopic equivalent strain and the average rate of the equivalent strain of each phase:

$$\dot{\bar{\varepsilon}}^{(i)} = \sqrt{\frac{2}{3}\mathbf{D}^{p(i)} : \mathbf{D}^{p(i)}} = a^{(i)}\sqrt{\frac{2}{3}\mathbf{D}^p : \mathbf{D}^p} \quad \Rightarrow$$

$$\dot{\bar{\varepsilon}}^{(i)} = a^{(i)}\dot{\bar{\varepsilon}} \tag{2.46}$$

In addition, we assume that during an increment, or over time $t_n < t < t_{n+1}$, all the phases are perfectly plastic, thus, the flow stresses $\sigma_0^{(i)}$ are constant. The value of the flow stress of each phase is given by the following expression:

$$\sigma_0^{(i)} = (1-\beta)\sigma_0^{(i)}|_n + \beta\sigma_0^{(i)}|_{n+1}, \quad 0 \leq \beta \leq 1, \tag{2.47}$$

where $\sigma_0^{(i)}|_n = \sigma_y^{(i)}\left(\bar{\varepsilon}_0^{(i)}|_n\right)$ and $\sigma_0^{(i)}|_{n+1} = \sigma_y^{(i)}\left(\bar{\varepsilon}_0^{(i)}|_{n+1}\right)$

Therefore, it can be proven through the Homogenisation theory that, as all phases are perfectly plastic, the material is macroscopically perfectly plastic, too, during the increment. The macroscopic flow stress of the material is acquired by solving the optimisation problem, for certain values of the volume fractions $c^{(i)}$. As a result, the macroscopic flow stress of the composite material is given as $\tilde{\sigma}_0 = \tilde{\sigma}_0\left(c^{(i)}, \sigma_0^{(i)}\right)$. The equation of the yield condition is written as:

$$\Phi\left(\mathbf{s}, c^{(r)}, \sigma_0^{(r)}\right) = \sigma_e\left(\mathbf{s}\right) - \tilde{\sigma}_0\left(c^{(r)}, \sigma_0^{(r)}\right) = 0 \tag{2.48}$$

In conclusion, for finite displacements, the problem problem is summarized as the system of the following differential equations, for $t_n \leq t \leq t_{n+1}$:

Constitutive equations:

$$\dot{\mathbf{E}} = \dot{\mathbf{E}}^e + \dot{\mathbf{E}}^{in} \tag{2.49}$$

$$\dot{\mathbf{E}}^{in} = \left(\dot{\bar{\varepsilon}} + A(\sigma_e)\dot{f}\right)\hat{\mathbf{N}} + \frac{1}{3}\dot{\varepsilon}_v^p\boldsymbol{\delta} \tag{2.50}$$

$$\dot{\hat{\boldsymbol{\sigma}}} = \boldsymbol{\mathcal{L}}^e : \dot{\mathbf{E}}^e \tag{2.51}$$

$$\dot{\bar{\varepsilon}}^{(i)} = a^{(i)}\dot{\bar{\varepsilon}} \tag{2.52}$$

where

$$A(\sigma_e) = A_1 + A_0\frac{\sigma_e}{s_a^*}, \quad \dot{\varepsilon}_v^p = \Delta_v\dot{f}, \quad a^{(i)} = a^{(i)}\left(c^{(r)}, \bar{\varepsilon}^{(i)}\right). \tag{2.53}$$

Equations of the evolution of the volume fractions:

$$\dot{c}^{(3)} = \dot{f} = c^{(2)} A_f \dot{\bar{\varepsilon}}^{(2)} \tag{2.54}$$

$$\dot{c}^{(1)} = -c^{(1)} \Delta_v \dot{f} = c^{(2)} A_f \dot{\bar{\varepsilon}}^{(2)} \tag{2.55}$$

$$\dot{c}^{(2)} = -\left(\dot{c}^{(1)} + \dot{f}\right) \tag{2.56}$$

where

$$A_f = A_f(\bar{\varepsilon}^{(2)}, \Sigma) = v_p(f) k m \left[N - N_v^{\varepsilon 0}\left(\bar{\varepsilon}^{(2)}\right)\right] \left(\bar{\varepsilon}^{(2)}\right)^{m-1} \exp\left(-a_\varepsilon n^*\right) \tag{2.57}$$

and

$$N_v^{\varepsilon 0} = N_v^{\varepsilon 0}\left(\bar{\varepsilon}^{(2)}\right), \quad n^* = n^*(\sigma_e). \tag{2.58}$$

As we have already mentioned, at any Gauss point, $\mathbf{F}_n$, $\boldsymbol{\sigma}_n$, $c_n^{(i)}$, $\bar{\varepsilon}_n^{(i)}$ and $\mathbf{F}_{n+1}$ are known, and $\boldsymbol{\sigma}_{n+1}$, $c_{n+1}^{(i)}$ and $\bar{\varepsilon}_{n+1}^{(i)}$ have to be determined. For this purpose, we use a combination of Backward and Forward Euler integration methods.

At this point it should be noted that equation (2.50) that determines the inelastic deformation rate $\dot{\mathbf{E}}^{in}$ and equation (2.54) that defines the evolution of the volume fraction of martensite f , as well as equation (2.52) require numerical integration. The rest of the equations are integrated exactly:

$$\Delta\mathbf{E} = \Delta\mathbf{E}^e + \Delta\mathbf{E}^{in} \quad \Rightarrow \quad \Delta\mathbf{E}^e = \Delta\mathbf{E} - \Delta\mathbf{E}^{in} \tag{2.59}$$

$$\hat{\sigma}_{n+1} = \sigma_n + \boldsymbol{\mathcal{L}}^e : \Delta\mathbf{E}^e = \sigma_n + \boldsymbol{\mathcal{L}}^e : \left(\Delta\mathbf{E} - \Delta\mathbf{E}^{in}\right) = \hat{\sigma}^e - \boldsymbol{\mathcal{L}}^e : \Delta\mathbf{E}^{in} \tag{2.60}$$

$$c_{n+1}^{(1)} = c_n^{(1)} \exp(-\Delta_v \Delta f) \tag{2.61}$$

$$c_{n+1}^{(a)} = -\left(c_{n+1}^{(1)} + c_{n+1}^{(m)}\right) \tag{2.62}$$

where $\hat{\boldsymbol{\sigma}}^e = \hat{\boldsymbol{\sigma}}_n + \boldsymbol{\mathcal{L}}^e : \Delta\mathbf{E}$ is the elastic predictor.
The remaining equations are

$$\dot{\mathbf{E}}^{in} = \left(\dot{\bar{\varepsilon}} + A(\sigma_e)\dot{f}\right)\hat{\mathbf{N}} + \frac{1}{3}\dot{\varepsilon}_v^p \boldsymbol{\delta} \tag{2.63}$$

$$\dot{\bar{\varepsilon}}^{(i)} = a^{(i)} \dot{\bar{\varepsilon}} \tag{2.64}$$

and

$$\dot{f} = c^{(2)} A_f \dot{\bar{\varepsilon}}^{(2)} \tag{2.65}$$

For the integration of the aforementioned constitutive equations we use the backward Euler method for the numerical integration of the "plastic flow" equation (2.63), and the forward Euler method for (2.65):

$$\Delta\mathbf{E}^{in} = \left(\Delta\bar{\varepsilon} + A_{n+1}\Delta f\right)\hat{\mathbf{N}}_{n+1} + \frac{1}{3}\Delta\varepsilon_v^p \boldsymbol{\delta}, \tag{2.66}$$

where $A_{n+1}(\sigma_e|_{n+1}) = A_0 + A_1 \frac{\sigma_e|_{n+1}}{s_a^*}$.

The evolution of the equivalent plastic strain in the phases (2.64) and of the volume fraction of the martensite (2.65) using the forward Euler scheme are written also as:

$$\Delta\bar{\varepsilon}^{(i)} = a_n^{(i)}\Delta\bar{\varepsilon} \tag{2.67}$$

$$\Delta f = c_n^{(2)} A_f|_n \Delta\bar{\varepsilon}^{(i)} = c_n^{(2)} A_f|_n a_n^{(i)} \Delta\bar{\varepsilon} \tag{2.68}$$

where $A_f|_n = v_p(f_n) km \left[N - N_v^{\varepsilon 0}\left(\bar{\varepsilon}_n^{(2)}\right)\right]\left(\bar{\varepsilon}_n^{(2)}\right)^{m-1} \exp\left(-a_\varepsilon n^*\right)$.

By substituting the expression for $\Delta\mathbf{E}^{in}$ from (3.17) in the elasticity equation:

$$\begin{aligned}\hat{\boldsymbol{\sigma}}|_{n+1} &= \hat{\boldsymbol{\sigma}}^e - (2\mu\ \mathcal{K} + 3\,\kappa\ \mathcal{J}) : \left[(\Delta\bar{\varepsilon} + A_{n+1}\,\Delta f)\,\hat{\mathbf{N}}_{n+1} + \frac{1}{3}\,\Delta\,\varepsilon_v^p\,\boldsymbol{\delta}\right] = \\ &= \hat{\boldsymbol{\sigma}}^e - 2\,\mu\,(\Delta\bar{\varepsilon} + A_{n+1}\,\Delta f)\,\hat{\mathbf{N}}_{n+1} - \kappa\,\Delta\varepsilon_v^p\,\boldsymbol{\delta}.\end{aligned} \tag{2.69}$$

From the previous equation, we split the stress tensor in two parts, the deviatoric and the spherical part:

$$\hat{\mathbf{s}}|_{n+1} = \hat{\mathbf{s}}|^e - 2\mu\,(\Delta\bar{\varepsilon} + A_{n+1}\Delta f)\,\hat{\mathbf{N}}_{n+1} \tag{2.70}$$

$$\hat{p}|_{n+1}\boldsymbol{\delta} = (\hat{p}^e - \kappa\Delta\varepsilon_v^p)\,\boldsymbol{\delta} \tag{2.71}$$

We use the relation $\Delta f = \Delta\varepsilon_v^p/\Delta_v$ to express $\hat{\mathbf{s}}|_{n+1}$ in terms of $\Delta\bar{\varepsilon}$ and $\Delta\varepsilon_v^p$:

$$\hat{\mathbf{s}}|_{n+1} = \hat{\mathbf{s}}^e - 2\mu\left(\Delta\bar{\varepsilon} + A_{n+1}\frac{\Delta\varepsilon_v^p}{\Delta_v}\right)\hat{\mathbf{N}}_{n+1}. \tag{2.72}$$

We can prove that $\hat{\mathbf{N}}_{n+1}$ is known as $\hat{\mathbf{N}}_{n+1} = \hat{\mathbf{N}}^e$, as they are both derived from tensors that have the same direction. We can show that $\hat{\mathbf{s}}|_{n+1}$ and $\hat{\mathbf{s}}^e$ are co-linear using the definition of $\hat{\mathbf{N}}_{n+1} \equiv \frac{3}{2\sigma_e|_{n+1}}\hat{s}_{n+1}$ in equation (2.72), and solve for $\hat{\mathbf{s}}_{n+1}$:

$$\hat{\mathbf{s}}_{n+1} = \frac{\hat{\mathbf{s}}^e}{1 + \mu\left(\Delta\bar{\varepsilon} + A_{n+1}\frac{\Delta\varepsilon_v^p}{\Delta_v}\right)\frac{3}{\sigma_e|_{n+1}}}. \tag{2.73}$$

Now we use the definition of equivalent stress $\sigma_e \equiv \sqrt{\frac{3}{2}\mathbf{s} : \mathbf{s}}$ and we substitute $\hat{\mathbf{s}}_{n+1}$, using the previous equation, in the first equation:

$$\left.\begin{aligned}\hat{\mathbf{N}}_{n+1} &\equiv \frac{3}{2\sqrt{\frac{3}{2}\hat{\mathbf{s}}_{n+1}:\hat{\mathbf{s}}_{n+1}}}\hat{\mathbf{s}}_{n+1} \\ \hat{\mathbf{N}}^e &\equiv \frac{3}{2\sqrt{\frac{3}{2}\hat{\mathbf{s}}^e:\hat{\mathbf{s}}^e}}\hat{\mathbf{s}}^e\end{aligned}\right\} \Rightarrow \hat{\mathbf{N}}_{n+1} = \hat{\mathbf{N}}^e. \tag{2.74}$$

The von Mises equivalent stress σ_e of a stress tensor $\boldsymbol{\sigma}$ is acquired by projecting this tensor to its corresponding $\mathbf{N}$ tensor:

$$\sigma_e{}^2 = \frac{3}{2}\mathbf{s} : \mathbf{s} = \sigma_e\mathbf{N} : \mathbf{s} \quad \Rightarrow \quad \sigma_e = \mathbf{s} : \mathbf{N} \tag{2.75}$$

As N is a deviatoric tensor and $\mathbf{s}$ is the deviatoric part of $\boldsymbol{\sigma}$, we write that:

$$\sigma_e = \mathbf{s} : \mathbf{N} = \boldsymbol{\sigma} : \mathbf{N}. \tag{2.76}$$

Therefore, we find $\sigma_e|_{n+1}$ by projecting $\hat{\mathbf{s}}_{n+1}$ to $\hat{\mathbf{N}}_{n+1}$:

$$\sigma_e|_{n+1} = \hat{\mathbf{s}}_{n+1} : \hat{\mathbf{N}}_{n+1} = \hat{\mathbf{s}}^e : \hat{\mathbf{N}}_{n+1} - 2\mu \left(\Delta\bar{\varepsilon} + A_{n+1} \frac{\Delta\varepsilon_v^p}{\Delta_v} \right) \hat{\mathbf{N}}_{n+1} : \hat{\mathbf{N}}_{n+1}. \tag{2.77}$$

Also, from equation (2.74) we know that $\hat{\mathbf{N}}_{n+1} = \hat{\mathbf{N}}^e$, so:

$$\hat{\mathbf{s}}_e : \hat{\mathbf{N}}_{n+1} = \hat{\mathbf{s}}_e : \hat{\mathbf{N}}^e = \sigma_e^e. \tag{2.78}$$

Considering the equation above, equation (2.77) and the definition of $A_{n+1} = A_0 + A_1 \frac{\sigma_e|_{n+1}}{s_a^*}$ we derive the following expression for $\sigma_e|_{n+1}$:

$$\sigma_e|_{n+1} = \sigma_e^e - 3\mu \left[\Delta\bar{\varepsilon} + \left(A_0 + A_1 \frac{\sigma_e|_{n+1}}{s_a^*} \right) \frac{\Delta\varepsilon_v^p}{\Delta_v} \right] \quad \Rightarrow$$

$$\sigma_e|_{n+1} = \frac{\sigma_e^e - 3\mu \left(\Delta\bar{\varepsilon} + A_0 \frac{\Delta\varepsilon_v^p}{\Delta_v} \right)}{1 + 3\mu \frac{A_1}{s_a^*} \frac{\Delta\varepsilon_v^p}{\Delta_v}}. \tag{2.79}$$

At this point, we write the equations (2.48) and (2.68) in terms of $\Delta\bar{\varepsilon}$ and $\Delta\varepsilon_v^p$:

$$\sigma_e|_{n+1} - \tilde{\sigma}_0|_{n+1} = \frac{\sigma_e^e - 3\mu \left(\Delta\bar{\varepsilon} + A_0 \frac{\Delta\varepsilon_v^p}{\Delta_v} \right)}{1 + 3\mu \frac{A_1}{s_a^*} \frac{\Delta\varepsilon_v^p}{\Delta_v}} - \tilde{\sigma}_0|_{n+1} = 0 \quad \Rightarrow$$

$$\sigma_e^e - 3\mu \left(\Delta\bar{\varepsilon} + A_0 \frac{\Delta\varepsilon_v^p}{\Delta_v} \right) - \left(1 + 3\mu \frac{A_1}{s_a^*} \frac{\Delta\varepsilon_v^p}{\Delta_v} \right) \tilde{\sigma}_0|_{n+1} = 0, \tag{2.80}$$

$$\Delta\varepsilon_v^p - \Delta_v c_n^{(2)} A_f|_n a_n^{(2)} \Delta\bar{\varepsilon} = 0. \tag{2.81}$$

Equations (2.80) and (2.81) consist a non-linear system of two equation, which has to be solved for $\Delta\bar{\varepsilon}$ and $\Delta\varepsilon_v^p$:

$$F_1 \left(\Delta\bar{\varepsilon}, \Delta\varepsilon_v^p \right) = \sigma_e^e - 3\mu \left(\Delta\bar{\varepsilon} + A_0 \frac{\Delta\varepsilon_v^p}{\Delta_v} \right) - \left(1 + 3\mu \frac{A_1}{s_a^*} \frac{\Delta\varepsilon_v^p}{\Delta_v} \right) \tilde{\sigma}_0|_{n+1} = 0 \tag{2.82}$$

$$F_2 \left(\Delta\bar{\varepsilon}, \Delta\varepsilon_v^p \right) = \Delta\varepsilon_v^p - \Delta_v c_n^{(2)} A_f|_n a_n^{(2)} \Delta\bar{\varepsilon} = 0. \tag{2.83}$$

We use the Newton Method to solve this system. The first estimates for $\Delta\bar{\varepsilon}$ and $\Delta\varepsilon_v^p$ are given in the next section. So, the values of $\Delta\bar{\varepsilon}$ and $\Delta\varepsilon_v^p$ in the first iteration of the newton loop will be:

$$\Delta\bar{\varepsilon} = a_1 \hat{\mathbf{N}} : \Delta\mathbf{E}, \tag{2.84}$$

where $a_1 = \dfrac{2}{3D}$, $D = 1 + \dfrac{H_n}{3\mu} + \mu \left(\dfrac{A_n}{\Delta_v} + \dfrac{H_v|_n}{3\mu} \right)$, $H_n = \displaystyle\sum_{i=1}^{3} \left(\frac{\partial \tilde{\sigma}_0}{\partial \sigma_0^{(i)}} \bigg|_n h_n^{(i)} a_n^{(i)} \right)$ and $H_v|_n = \displaystyle\sum_{i=1}^{3} \left(\frac{\partial \tilde{\sigma}_0}{\partial c^{(i)}} \bigg|_n g_n^{(i)} \right)$,
and

$$\Delta\varepsilon_v^p = m d\bar{\varepsilon} = m a_1 \hat{\mathbf{N}} : \Delta\mathbf{E}, \tag{2.85}$$

where $m = \Delta_v c_n^{(2)} a_n^{(2)} A_n$ and $a^{(i)}$ are known from the previous increment. More details on these quantities will be given in the following section.
Within each iteration in the Newton loop, for given $\Delta\bar{\varepsilon}$ and $\Delta\varepsilon_v^p$, we calculate the following:

$$c_{n+1}^{(1)} = c_n^{(1)} \exp\left(-\Delta\varepsilon_v^p\right)$$
$$c_{n+1}^{(3)} = c_n^{(3)} + \frac{\Delta\varepsilon_v^p}{\Delta_v}$$
$$c_{n+1}^{(2)} = 1 - \left(c_{n+1}^{(1)} + c_{n+1}^{(3)}\right)$$
$$\Delta\bar{\varepsilon}_{(i)} = a_n^{(i)} \Delta\bar{\varepsilon},$$

where $a_n^{(i)}$ are known from the solution of the optimization problem of the previous increment. As $c_{n+1}^{(i)}$ and $\bar{\varepsilon}_{n+1}^{(i)} = \bar{\varepsilon}_n^{(i)} + \Delta\bar{\varepsilon}^{(i)}$ are known, we are able through the Homogenization theory to determine:

$$\tilde{\sigma}_0|_{n+1} = \tilde{\sigma}_0\left(c_{n+1}^{(i)}, \bar{\varepsilon}_{n+1}^{(i)}\right).$$

Finally, we can compute σ_e^e, using the definition of von Mises equivalent stress, and $A_f|_n = A_f\left(\bar{\varepsilon}_n^{(2)}, \Sigma_n\right)$ from (2.57):

$$\sigma_e^e = \sqrt{\frac{3}{2}\hat{\mathbf{s}}_{n+1} : \hat{\mathbf{s}}_{n+1}} \quad ,$$

$$A_f|_n = A_f(\bar{\varepsilon}_n, \Sigma_n) = v_p(f_n) k m \left[N - N_v^{\varepsilon 0}\left(\bar{\varepsilon}_n^{(2)}\right)\right]\left(\bar{\varepsilon}_n^{(2)}\right)^{m-1} \exp\left(-a_\varepsilon n^*\right),$$

where $\Sigma_n = \frac{p_n}{\sigma_e|_n}$.

As we have found all the quantities involved in the system of equations (2.82) and (2.83), we can now calculate the Jacobian matrix for the Newton Loop:

$$\mathbf{J} = \begin{bmatrix} J_{11} J_{12} \\ J_{21} J_{22} \end{bmatrix},$$

where:

$$J_{11} = \frac{\partial F_1}{\partial \Delta\bar{\varepsilon}} = -3\mu - \left(1 + \frac{3G}{s_a^*}\frac{A_1}{\Delta_v}\Delta\varepsilon_v^p\right)\sum_1^3 \frac{\partial\tilde{\sigma}_0}{\partial\sigma_0^{(i)}} h^{(i)} a_n^{(i)} \tag{2.86}$$

$$J_{12} = \frac{\partial F_1}{\partial \Delta\varepsilon_v^p} = -3\mu\left(\frac{A_0}{\Delta_v} + \frac{A_1}{\Delta_v}\frac{\bar{\sigma}_0|_{n+1}}{s_a^*}\right) - \left(1 + 3\mu\frac{A_1}{s_a^*\Delta_v}\Delta\varepsilon_v^p\right)\sum_{i=1}^3 \frac{\partial\tilde{\sigma}_0}{\partial c^{(i)}}\frac{\partial c^{(i)}}{\partial\Delta\varepsilon_v^p} \tag{2.87}$$

$$J_{21} = \frac{\partial F_2}{\partial \Delta\bar{\varepsilon}} = -\Delta_v c_n^{(2)} A_f|_n a_n^{(2)} \tag{2.88}$$

$$J_{22} = \frac{\partial F_2}{\partial \Delta\varepsilon_v^p} = 1 \tag{2.89}$$

The derivatives $\frac{\partial\tilde{\sigma}_0}{\partial\sigma_0^{(i)}}$ and $\frac{\partial\tilde{\sigma}_0}{\partial c^{(i)}}$ are obtained from the Homogenisation Theory.

The definitions of $h^{(i)}$ and $a_n^{(i)}$ are:

$$h^{(i)} = \frac{\partial\sigma_0^{(i)}}{\partial\bar{\varepsilon}^{(i)}},$$

$$a_n^{(i)} = \frac{\partial \Delta\bar{\varepsilon}_{(i)}}{\partial \Delta\bar{\varepsilon}} = \frac{\partial \bar{\varepsilon}_{(i)}}{\partial \bar{\varepsilon}},$$

We also need the following derivatives :

$$\frac{\partial c_{n+1}^{(1)}}{\partial \Delta\varepsilon_v^p} = -c_{n+1}^{(1)} \tag{2.90}$$

$$\frac{\partial c_{n+1}^{(3)}}{\partial \Delta\varepsilon_v^p} = \frac{1}{\Delta_v} \tag{2.91}$$

$$\frac{\partial c_{n+1}^{(2)}}{\partial \Delta\varepsilon_v^p} = c_{n+1}^{(1)} - \frac{1}{\Delta_v} \tag{2.92}$$

Details on the Jacobian matrix and these derivatives are presented explicitly in the appendices.

2.3 The Linearization moduli

When the finite element method is used for the solution to the problem, we need to calculate the linearization moduli:

$$\mathbf{C} = \frac{\partial \boldsymbol{\sigma}}{\partial \mathbf{E}}$$

$$\hat{\mathbf{C}} = \frac{\partial \hat{\boldsymbol{\sigma}}_{n+1}}{\partial \mathbf{E}_{n+1}}$$

$$C_{ijkl} \simeq R_{im}|_{n+1} R_{jn}|_{n+1} R_{kp}|_{n+1} R_{lq}|_{n+1} \hat{C}_{mnpq}$$

Generally, $\mathbf{C}$ depends not only on the constitutive model but also on the algorithm used for the numerical integration of the constitutive equations. The equation that defines $\hat{\boldsymbol{\sigma}}_{n+1}$ is:

$$\hat{\boldsymbol{\sigma}}_{n+1} = \hat{\boldsymbol{\sigma}}_n + \boldsymbol{\mathcal{L}}^e : \Delta\mathbf{E}^e = \hat{\boldsymbol{\sigma}}_n + \boldsymbol{\mathcal{L}}^e : \left(\Delta\mathbf{E} - \Delta\mathbf{E}^{in}\right)$$

By differentiating this equation and using equation (2.45) for $d\mathbf{E}^{in}$:

$$d\hat{\boldsymbol{\sigma}}_{n+1} = \boldsymbol{\mathcal{L}}^e : d\mathbf{E}^e = \boldsymbol{\mathcal{L}}^e : d\mathbf{E} - \boldsymbol{\mathcal{L}}^e : d\mathbf{E}^{in} =$$
$$= \boldsymbol{\mathcal{L}}^e : d\mathbf{E} - \boldsymbol{\mathcal{L}}^e : \left[\left(d\bar{\varepsilon} + A_{n+1}\frac{d\varepsilon_v^p}{\Delta_v}\right)\hat{\mathbf{N}}_{n+1} + \frac{1}{3}d\varepsilon_v^p\boldsymbol{\delta}\right] =$$

$$= \boldsymbol{\mathcal{L}}^e : d\mathbf{E} - 2\mu\left(d\bar{\varepsilon} + A_{n+1}\frac{d\varepsilon_v^p}{\Delta_v}\right)\hat{\mathbf{N}}_{n+1} - \kappa d\varepsilon_v^p\boldsymbol{\delta} \tag{2.93}$$

In order to find the linearization moduli we have to express $d\bar{\varepsilon}$ and $d\varepsilon_v^p$ in terms of $d\mathbf{E}$. We begin with the calculation of $d\varepsilon_v^p$. Equation (2.83) suggests that:

$$d\varepsilon_v^p = \Delta_v c^{(2)} a^{(2)} A_f|_n d\bar{\varepsilon}$$

or

$$d\varepsilon_v^p = m d\bar{\varepsilon}, \tag{2.94}$$

with $m = \Delta_v c^{(2)} a^{(2)} A_f|_n$.

The consistency condition suggests that:

$$d\Phi\left(\hat{\mathbf{s}}, \bar{\varepsilon}^{(i)}, c^{(i)}\right) = 0 \Rightarrow$$

$$\hat{\mathbf{N}} : d\hat{\mathbf{s}} - \sum_{i=1}^{3}\left(\frac{\partial\tilde{\sigma}_0}{\partial\bar{\varepsilon}^{(i)}} d\bar{\varepsilon}^{(i)} + \frac{\partial\tilde{\sigma}_0}{\partial c^{(i)}} dc^{(i)}\right) = 0 \quad \Rightarrow$$

$$2\mu\hat{\mathbf{N}} : d\mathbf{E} - 3\mu\left(d\bar{\varepsilon} + \frac{A}{\Delta_v} d\varepsilon_v^p\right) - d\bar{\varepsilon}\sum_{i=1}^{3}\left(\frac{\partial\tilde{\sigma}_0}{\partial\sigma_0^{(i)}} h^{(i)} a^{(i)}\right) - d\varepsilon_v^p \sum_{i=1}^{3}\left(\frac{\partial\tilde{\sigma}_0}{\partial c^{(i)}} g^{(i)}\right) = 0, \tag{2.95}$$

where we tok into consideration that $\hat{\mathbf{N}} : d\hat{\mathbf{s}} = \hat{\mathbf{N}} : d\hat{\boldsymbol{\sigma}}$ and $\hat{\mathbf{N}} : \boldsymbol{\delta} = 0$. We have also used the expression (2.93) for $d\hat{\boldsymbol{\sigma}}$.

Next, we substitute $d\varepsilon_v^p$ in the previous equation:

$$d\bar{\varepsilon} = \frac{2\mu}{3\mu + H + m\left(3\mu\frac{A}{\Delta_v} + H_v\right)} \hat{\mathbf{N}} : d\mathbf{E}$$

or

$$d\bar{\varepsilon} = a_1 \hat{\mathbf{N}} : d\mathbf{E}, \tag{2.96}$$

with $a_1 = \dfrac{2}{3D}$, $D = 1 + \dfrac{H}{3\mu} + \mu\left(\dfrac{A}{\Delta_v} + \dfrac{H_v}{3\mu}\right)$, $H = \displaystyle\sum_{i=1}^{3}\left(\frac{\partial\tilde{\sigma}_0}{\partial\sigma_0^{(i)}} h^{(i)} a^{(i)}\right)$ and $H_v = \displaystyle\sum_{i=1}^{3}\left(\frac{\partial\tilde{\sigma}_0}{\partial c^{(i)}} g^{(i)}\right)$.

Therefore $d\mathbf{E}^{in}$ can be written in the following form:

$$d\mathbf{E}^{in} = \left(d\bar{\varepsilon} + \frac{A}{\Delta_v} d\varepsilon_v^p\right)\hat{\mathbf{N}} + \frac{1}{3} d\varepsilon_v^p\,\delta = a_1\left(1 + \frac{A}{\Delta_v} m\right)\hat{\mathbf{N}}\,\hat{\mathbf{N}} : d\mathbf{E} + \frac{1}{3} a_1\, m\,\delta\mathbf{N} : d\mathbf{E} \tag{2.97}$$

Finally, we substitute $d\mathbf{E}^{in}$ from (2.97) into (2.93) to derive

$$\begin{aligned} d\hat{\boldsymbol{\sigma}} = \boldsymbol{\mathcal{L}}^e : d\mathbf{E} - 2\mu\left(a_1\hat{\mathbf{N}} : d\mathbf{E} + A\frac{m a_1 \hat{\mathbf{N}} : d\mathbf{E}}{\Delta_v}\right)\hat{\mathbf{N}} + \kappa m a_1 (\hat{\mathbf{N}} : d\mathbf{E})\boldsymbol{\delta} = \\ = \left(2\mu\boldsymbol{\mathcal{K}} + 3\kappa\boldsymbol{\mathcal{J}} - f_1\hat{\mathbf{N}}\hat{\mathbf{N}} - f_2\boldsymbol{\delta}\hat{\mathbf{N}}\right) : d\mathbf{E} \end{aligned} \tag{2.98}$$

so

$$\hat{\boldsymbol{\mathcal{C}}} = 2\mu\boldsymbol{\mathcal{K}} + 3\kappa\boldsymbol{\mathcal{J}} - f_1\hat{\mathbf{N}}\hat{\mathbf{N}} - f_2\boldsymbol{\delta}\hat{\mathbf{N}} \tag{2.99}$$

where $f_1 = 2\mu a_1\left(1 + \frac{A}{\Delta_v} m\right)$, $f_2 = \kappa m a_1$.

2.4 Implementation in UMAT subroutine

The constitutive model described above is implemented into the ABAQUS general purpose finite element code via the UMAT (User-MATerial) subroutine. UMAT can be called by the user to define the mechanical behavior of a material. UMAT is called at any material calculation point of elements for which the material definition includes a user-defined material behavior. For each increment, the user is provided with the deformation gradient ($\mathbf{F}_n$), the stresses ($\boldsymbol{\sigma}_n$) and all state dependent variables $\left(\bar{\varepsilon}_n, c_n^{(i)}, \bar{\varepsilon}_n^{(i)}, y_{in} = y_{in}(a_n^{(r)})\right)$, at the start of the increment, as well as the deformation gradient at the end of the increment, ($\mathbf{F}_{n+1}$). Given all those quantities, the user has to return the stresses ($\boldsymbol{\sigma}_{n+1}$) and all state dependent variables $\left(\bar{\varepsilon}_{n+1}, c_{n+1}^{(i)}, \bar{\varepsilon}_{n+1}^{(i)}, y_{in} = y_{in+1}(a_{n+1}^{(r)})\right)$ at the end of the increment. A UMAT subroutine must also provide the material Jacobian matrix ($\partial\Delta\boldsymbol{\sigma}/\partial\Delta\mathbf{E}$) corresponding to the mechanical constitutive model under consideration.

The basic variables predefined in a general UMAT subroutine are summarized in table 3.1. When developing a UMAT subroutine the user is also free to define solution-dependent state variables (STATEV) and ABAQUS will store their values at the end of every increment, making them available for future calculations on subsequent increments. Solution dependent variables need to be updated to their values at the end of every increment.

Table 2.1: Interpretation of the predefined variables in a UMAT subroutine

NDI	Number of direct stress components
NSHR	Number of shear stress components
NTENS	Number of total stress components (NDI + NSHR)
NPROPS	Number of material constants associated with this material (defined by user)
NSTATEV	Number of extra solution-depended state variables associate with this material (defined by user)
PROPS(NPROPS)	Array of material constants (user defined)
STRESS(NTENS)	Array containing the true or Cauchy stress components
STATEV(NSTATEV)	Array containing the solution-depended state variables
STRAN(NTENS)	Array containing the total strains
DSTRAN(NTENS)	Array containing the strain increments
DDSDDE(NTENS,NTENS)	Jacobian matrix of the constitutive model
DROT(3,3)	Rotation increment matrix
DFGRD0(3,3)	Deformation gradient at the beginning of the increment
DFGRD1(3,3)	Deformation gradient at the end of the increment
CMNAME	Name of the user-defined material

We have 18 constant quantities associated with the properties of the material, so NPROPS = 18. These quantities are contained in the array PROPS(18). The array of the properties is presented in table 2.4, below:

Table 2.2: Constants used in the model

E	Young's modulus
v	Poisson's ratio
N_{phases}	Number of phases
A_0	Constant
A_1	Constant
s_a^*	Reference austenite stress
Δ_v	Relative volume change caused by martensitic transformation
v_p	average volume of austenite particles
k	Constant
m	Constant
N	Maximum number of nucleation sites can be produced by plastic strain
a_ε	Shape factor of strain modified potency distribution
E_{str}	Elastic strain energy
γ_s	Fault/matrix inter-facial energy
ρ	Density of atoms
T	Temperature
X_{Mn}	Mole fraction of Mn
X_C	Mole fraction of C

Also, we have 12 state dependent variables, contained in the array STATEV(12), as presented in the table 2.4.

Table 2.3: State depended variables

$\bar{\varepsilon}$	Equivalent plastic strain
a	Elastic flag (0 for elasticity, 1 for plasticity)
Σ	Stress triaxility
$c^{(i)}, i = 1, 2, 3$	Volume fractions of ferrite, austenite and martensite, respactively
$\bar{\varepsilon}^{(i)}, i = 1, 2, 3$	Average equivalent plastic strains of each phase
$y^{(i)}$	Optimisation parameters

Chapter 3

Computational model for Plane Stress

In this chapter, we develop a model for a plane stress analysis. In a general deformation driven analysis, displacement is considered as known and we have to compute the stress tensor. In contrast, in plane stress, we consider a thin plate with its center lying on plane, where the out of plane strain components are not defined kinematically and the out of plain stress components are zero. The concept is fundamentally the same, but the deformation gradient component F_{33} is unknown and the stress component σ_{33} is zero, so it is considered to be known. The deformation gradient, in matrix form is:

$$\mathbf{F} = \begin{bmatrix} F_{11} & F_{12} & 0 \\ F_{21} & F_{22} & 0 \\ 0 & 0 & F_{33} \end{bmatrix},$$

where F_{33} is unknown, while the stress tensor has the form:

$$\boldsymbol{\sigma} = \begin{bmatrix} \sigma_{11} & \sigma_{12} & 0 \\ \sigma_{21} & \sigma_{22} & 0 \\ 0 & 0 & 0 \end{bmatrix}.$$

So, in this problem, F_{33} is an unknown variable, and σ_{33} is known. As a result, during an increment, one part of $\mathbf{F}_{n+1}$ is not defined kinematically. Thus, we will adopt the following implementation for $\Delta\mathbf{F} = \mathbf{F}_{n+1} - \mathbf{F}_n$:

$$\Delta\mathbf{F} = \begin{bmatrix} \Delta\bar{F}_{11} & \Delta\bar{F}_{12} & 0 \\ \Delta\bar{F}_{21} & \Delta\bar{F}_{22} & 0 \\ 0 & 0 & \Delta F_{33} \end{bmatrix},$$

where $\Delta\bar{F}_{\alpha\beta}$, $\alpha, \beta = (1, 2)$ are the known in-plane components and ΔF_{33} is the unknown out-of-plane component. For this deformation gradient tensor $\Delta\mathbf{F}$, we have its corresponding right stretch and orthogonal rotation tensors and the logarithmic stretch tensor:

$$\Delta\mathbf{U} = \begin{bmatrix} \Delta\bar{U}_{11} & \Delta\bar{U}_{12} & 0 \\ \Delta\bar{U}_{21} & \Delta\bar{U}_{22} & 0 \\ 0 & 0 & \Delta U_{33} \end{bmatrix}, \tag{3.1}$$

$$\Delta\mathbf{R} = \begin{bmatrix} \Delta\bar{R}_{11} & \Delta\bar{R}_{12} & 0 \\ \Delta\bar{R}_{21} & \Delta\bar{R}_{22} & 0 \\ 0 & 0 & 1 \end{bmatrix} \tag{3.2}$$

and

$$\Delta\mathbf{E} = \begin{bmatrix} \Delta\bar{E}_{11} & \Delta\bar{E}_{12} & 0 \\ \Delta\bar{E}_{21} & \Delta\bar{E}_{22} & 0 \\ 0 & 0 & \Delta E_{33} \end{bmatrix}, \tag{3.3}$$

where $\Delta\bar{\mathbf{U}}$ and $\Delta\bar{\mathbf{R}}$ can be computed through Polar Decomposition of the known part of $\Delta\mathbf{F}$ tensor:

$$\Delta\bar{\mathbf{F}} = \begin{bmatrix} \Delta\bar{F}_{11} & \Delta\bar{F}_{12} & 0 \\ \Delta\bar{F}_{21} & \Delta\bar{F}_{22} & 0 \\ 0 & 0 & 0 \end{bmatrix},$$

so, the known part of the logarithmic strain tensor $\Delta\bar{\mathbf{E}}$ is:

$$\Delta\bar{\mathbf{E}} = \begin{bmatrix} \Delta\bar{E}_{11} & \Delta\bar{E}_{12} & 0 \\ \Delta\bar{E}_{21} & \Delta\bar{E}_{22} & 0 \\ 0 & 0 & 0 \end{bmatrix} = \ln\bar{\mathbf{U}}.$$

For convenience, we adopt the following expression for $\Delta\mathbf{E}$:

$$\Delta\mathbf{E} = \Delta\bar{\mathbf{E}} + \Delta E_{33}\mathbf{a}, \tag{3.4}$$

where $\mathbf{a} = \mathbf{e}_3\mathbf{e}_3$. As a result, the deviatoric part of $\mathbf{a}'$ is:

$$\mathbf{a}' = \mathbf{e}_3\mathbf{e}_3 - \frac{1}{3}\boldsymbol{\delta} = -\frac{1}{3}\left(\mathbf{e}_1\mathbf{e}_3 + \mathbf{e}_1\mathbf{e}_1 - 2\mathbf{e}_3\mathbf{e}_3\right) \tag{3.5}$$

The component ΔE_{33}, which is unknown is determined from the plane stress condition:

$$\sigma_{33} = \mathbf{e}_3 \cdot \sigma \cdot \mathbf{e}_3 = 0. \tag{3.6}$$

3.1 Numerical Integration of the Constitutive Equations

As we are dealing with the same material, we are using the constitutive equations developed in Chapter 2.

Constitutive equations:

$$\dot{\mathbf{E}} = \dot{\mathbf{E}}^e + \dot{\mathbf{E}}^{in} \tag{3.7}$$

$$\dot{\boldsymbol{\sigma}} = \boldsymbol{\mathcal{L}}^e : \dot{\mathbf{E}}^e \tag{3.8}$$

$$\dot{\mathbf{E}}^{in} = \left(\dot{\bar{\varepsilon}} + \frac{A}{\Delta_v}\dot{\varepsilon}_v^p\right)\hat{\mathbf{N}} + \frac{1}{3}\dot{\varepsilon}_v^p\boldsymbol{\delta} \tag{3.9}$$

$$\dot{\bar{\varepsilon}}^{(i)} = a^{(i)}\dot{\bar{\varepsilon}} \tag{3.10}$$

The yield condition:

$$\Phi\left(\mathbf{s}, c^{(i)}, \bar{\varepsilon}^{(i)}\right) = \sigma_e(\mathbf{s}) - \tilde{\sigma}_0\left(c^{(i)}, \bar{\varepsilon}^{(i)}\right) = 0 \tag{3.11}$$

The evolution equations of the volume fractions of the constituent phases are defined by the following equations:

$$\dot{c}^{(1)} = -c^{(1)}\dot{\varepsilon}_v^p \equiv \dot{\varepsilon}_v^p g^{(1)} \tag{3.12}$$

$$\dot{c}^{(3)} = \dot{f} = c^{(2)} A_f \dot{\bar{\varepsilon}}^{(2)} \tag{3.13}$$

$$\dot{c}^{(2)} = -\left(\dot{c}^{(1)} + \dot{c}^{(3)}\right) = \left(c^{(1)} - \frac{1}{\Delta_v}\right)\dot{\varepsilon}_v^p \equiv \dot{\varepsilon}_v^p g^{(2)} \tag{3.14}$$

$$\dot{\varepsilon}_v^p = \Delta_v \dot{f} = \Delta_v c^{(2)} A_f \dot{\bar{\varepsilon}}^{(2)} \tag{3.15}$$

$$A_f = A_f(\bar{\varepsilon}^{(2)}, \Sigma) \tag{3.16}$$

The Backward Euler integration scheme is used for the plastic flow equation (3.9):

$$\Delta\mathbf{E}^{in} = \left(\Delta\bar{\varepsilon} + A_{n+1}\Delta f\right)\hat{\mathbf{N}}_{n+1} + \frac{1}{3}\Delta\varepsilon_v^p\boldsymbol{\delta} \tag{3.17}$$

where $A_{n+1} = A_0 + A_1\frac{\sigma_e|_{n+1}}{s_a^*}$.

Exact integration for (3.12), (3.13), (3.14) and (3.15):

$$\Delta\varepsilon_v^p = \Delta_v \Delta f \tag{3.18}$$

$$c_{n+1}^{(1)} = c_n^{(1)} \exp\left(-\Delta\varepsilon_v^p\right) \tag{3.19}$$

$$c_{n+1}^{(3)} = c_n^{(3)} + \frac{\Delta\varepsilon_v^p}{\Delta_v} \tag{3.20}$$

$$c_{n+1}^{(2)} = 1 - \left(c_{n+1}^{(1)} + c_{n+1}^{(3)}\right) \tag{3.21}$$

The Forward Euler integration scheme is used for equations (3.13) and (3.10):

$$\Delta f = c_n^{(3)} A_f|_n a_n^{(2)} \Delta\bar{\varepsilon} \tag{3.22}$$

where $A_f|_n = v_p\left(f_n\right) km\left[N - N_v^{e0}(\,\bar{\varepsilon}_n^{(2)}\,)\right]\left(\bar{\varepsilon}_n^{(2)}\right)^{m-1}\exp\left(-a_\varepsilon n^*\right)$

$$\Delta\bar{\varepsilon}^{(i)} = a_n^{(i)}\Delta\bar{\varepsilon} \tag{3.23}$$

The elasticity equation, using (3.4) expression for $\Delta\mathbf{E}$, becomes:

$$\begin{aligned}\hat{\boldsymbol{\sigma}}_{n+1} &= \hat{\boldsymbol{\sigma}}_n + \boldsymbol{\mathcal{L}}^e : \Delta\mathbf{E}^e = \hat{\boldsymbol{\sigma}}_n + \boldsymbol{\mathcal{L}}^e : \left(\Delta\mathbf{E} - \Delta\mathbf{E}^{in}\right) \\ &= \hat{\boldsymbol{\sigma}}_n + \boldsymbol{\mathcal{L}}^e : \left(\Delta\bar{\mathbf{E}} + \Delta E_{33}\mathbf{a} - \Delta\mathbf{E}^{in}\right) \\ &= \bar{\boldsymbol{\sigma}}^e + \boldsymbol{\mathcal{L}}^e : \left(\Delta E_{33}\mathbf{a} - \Delta\mathbf{E}^{in}\right).\end{aligned} \tag{3.24}$$

In addition, we substitute $\Delta\mathbf{E}^{in}$ using equations (3.17) and (3.22), and the definition of the elastic moduli, $\boldsymbol{\mathcal{L}}^e = 2\mu\boldsymbol{\mathcal{K}} + 3\kappa\boldsymbol{\mathcal{J}}$:

$$\hat{\boldsymbol{\sigma}}_{n+1} = \bar{\boldsymbol{\sigma}}^e + \boldsymbol{\mathcal{L}}^e : \left[\Delta E_{33}\mathbf{a} - \left(\Delta\bar{\varepsilon} + A_{n+1}\Delta f\right)\hat{\mathbf{N}}_{n+1} - \frac{1}{3}\Delta\varepsilon_v^p\boldsymbol{\delta}\right] =$$

$$= \bar{\boldsymbol{\sigma}}^e + (2\mu\boldsymbol{\mathcal{K}} + 3\kappa\boldsymbol{\mathcal{J}}) : \left[\Delta E_{33}\mathbf{a} - \left(\Delta\bar{\varepsilon} + \frac{A_{n+1}}{\Delta_v}\Delta\varepsilon_v^p\right)\hat{\mathbf{N}}_{n+1} - \frac{1}{3}\Delta\varepsilon_v^p\boldsymbol{\delta}\right]$$

$$= \bar{\boldsymbol{\sigma}}^e - 2\mu\left[\left(\Delta\bar{\varepsilon} + \frac{A_{n+1}}{\Delta_v}\Delta\varepsilon_v^p\right)\hat{\mathbf{N}}_{n+1} - \Delta E_{33}\mathbf{a}'\right] - \kappa\left(\Delta\varepsilon_v^p - \Delta E_{33}\right)\boldsymbol{\delta} \tag{3.25}$$

Having the the stress tensor written in this form , we calculate the deviatoric and the spherical parts of $\hat{\sigma}_{n+1}$:

$$\hat{s}_{n+1} = \bar{s}^e - 2\mu\left[\left(\Delta\bar{\varepsilon} + \frac{A_{n+1}}{\Delta_v}\right)\hat{\mathbf{N}}_{n+1} - \Delta E_{33}\mathbf{a}'\right] \tag{3.26}$$

and

$$\hat{p}_{n+1} = \bar{p}^e - \kappa\left(\Delta\varepsilon_v^p - \Delta E_{33}\right). \tag{3.27}$$

It has to be mentioned that $\bar{\sigma}^e = \hat{\sigma}_n + \boldsymbol{\mathcal{L}}^e : \Delta\bar{\mathbf{E}}$ is the elastic predictor corresponding to the "known" part of $\Delta\mathbf{E}$.

In equation (3.26) we use the definition of $\hat{\mathbf{N}}_{n+1} = \dfrac{3}{2\sigma_e|_{n+1}}\hat{\mathbf{s}}_{n+1}$ and solve for $\hat{\mathbf{s}}_{n+1}$:

$$\hat{s}_{n+1} = \bar{s}^e - 2\mu\left[\left(\Delta\bar{\varepsilon} + \frac{A_{n+1}}{\Delta_v}\right)\hat{\mathbf{N}}_{n+1} - \Delta E_{33}\mathbf{a}'\right] \Rightarrow$$

$$\hat{s}_{n+1} = \frac{\bar{\mathbf{s}}^e + 2\mu\Delta E_{33}\mathbf{a}'}{1 + \frac{3\mu}{\sigma_e|_{n+1}}\left(\Delta\bar{\varepsilon} + \frac{A_{n+1}}{\Delta_v}\Delta\varepsilon_v^p\right)}. \tag{3.28}$$

We should mention that in this case, in contrast with the previous model, $\hat{\mathbf{s}}_{n+1}$ and $\bar{\mathbf{s}}_{n+1}$ do not have the same direction. As a result, in general, $\hat{\mathbf{N}}_{n+1} \neq \bar{\mathbf{N}}^e$, where $\hat{\mathbf{N}}_{n+1}$ and $\bar{\mathbf{N}}^e$ are corresponding to $\hat{\mathbf{s}}_{n+1}$ and $\bar{\mathbf{s}}^e$ tensors, respectively.

At this point, we will derive an expression for the von Mises equivalent stress, as we have done in the previous model. We will use the definition of the equivalent stress $\left(\sigma_e|_{n+1}\right)^2 = \frac{3}{2}\hat{\mathbf{s}}_{n+1} : \hat{\mathbf{s}}_{n+1}$ and (3.28), so:

$$\left(\sigma_e|_{n+1}\right)^2 = \frac{3}{2}\frac{\bar{\mathbf{s}}^e : \bar{\mathbf{s}}^e + 4\mu\Delta E_{33}\bar{\mathbf{s}}^e : \mathbf{a}' + (2\mu\Delta E_{33})^2\mathbf{a}' : \mathbf{a}'}{\left[1 + \frac{3\mu}{\sigma_e|_{n+1}}\left(\Delta\bar{\varepsilon} + \frac{A_{n+1}}{\Delta_v}\Delta\varepsilon_v^p\right)\right]^2}$$

$$= \frac{(\bar{\sigma}_e^e)^2 + 6\mu\Delta E_{33}\bar{s}_{33}^e + (2\mu\Delta E_{33})^2}{\left[1 + \frac{3\mu}{\sigma_e|_{n+1}}\left(\Delta\bar{\varepsilon} + \frac{A_{n+1}}{\Delta_v}\Delta\varepsilon_v^p\right)\right]^2} \tag{3.29}$$

Finally, by using $A_{n+1} = A_0 + A_1\frac{\sigma_e|_{n+1}}{s_a^*}$ in the previous equation and solving for $\sigma_e|_{n+1}$ we obtain:

$$\left(\sigma_e|_{n+1}\right)^2 = \frac{(\bar{\sigma}_e^e)^2 + 6\mu\Delta E_{33}\bar{s}_{33}^e + (2\mu\Delta E_{33})^2}{\left[1 + \frac{3\mu}{\sigma_e|_{n+1}}\left(\Delta\bar{\varepsilon} + \frac{A_0 + A_1\frac{\sigma_e|_{n+1}}{s_a^*}}{\Delta_v}\Delta\varepsilon_v^p\right)\right]^2} \Rightarrow$$

$$\sigma_e|_{n+1} = \frac{\mu\left[\sqrt{\frac{\bar{\sigma}_e^e}{\mu^2} + \frac{6\Delta E_{33}\bar{s}_{33}^e}{\mu} + 4(\Delta E_{33})^2} - \left(\Delta\bar{\varepsilon} + \frac{A_0}{\Delta_v}\Delta\varepsilon_v^p\right)\right]}{1 + \frac{A_1}{\Delta_v}\frac{3\mu}{s_a^*}}. \tag{3.30}$$

We acquire in the following form for $\sigma_e|_{n+1}$, that can be substituted in the yield condition:

$$\sigma_e|_{n+1} = \frac{\mu\left[F\left(\Delta E_{33}\right) - \left(\Delta\bar{\varepsilon} + \frac{A_0}{\Delta_v}\Delta\varepsilon_v^p\right)\right]}{1 + \frac{A_1}{\Delta_v}\frac{3\mu}{s_a^*}}, \tag{3.31}$$

where $F\left(\Delta E_{33}\right) = \sqrt{\frac{\bar{\sigma}_e^e}{\mu^2} + \frac{6\Delta E_{33}\bar{s}_{33}^e}{\mu} + 4(\Delta E_{33})^2}$.

In this model, we have to solve a system of three equations, as we have an additional unknown quantity, ΔE_{33}. The third equation is the Plane stress condition, or:

$$\sigma_{33}|_{n+1} = 0 \tag{3.32}$$

Using equation (3.2) we find that:

$$\hat{\sigma}_{33}|_{n+1} = \mathbf{e}_3 \cdot \Delta\mathbf{R} \cdot \boldsymbol{\sigma}_{n+1} \cdot \Delta\mathbf{R} \cdot \mathbf{e}_3 = 0 \tag{3.33}$$

This equation has to be expressed in terms that can be computed for given values of the unknowns, $\Delta\bar{\varepsilon}$, $\Delta\varepsilon_v^p$ and ΔE_{33}. Firstly, we will write this equation as:

$$\hat{\sigma}_{33}|_{n+1} = \hat{s}_{33}|_{n+1} + \hat{p}_{n+1}$$

and we use equation (3.28), so:

$$\bar{s}_3^e 3 + \frac{4}{3}\mu\Delta E_{33} + \left[1 + \frac{3\mu}{\sigma_e|_{n+1}}\left(\Delta\bar{\varepsilon} + \frac{A_{n+1}}{\Delta_v}\Delta\varepsilon_v^p\right)\right]\hat{p}_{33}|_{n+1} = 0 \tag{3.34}$$

Finally, we get the following non-linear system of three equations,(3.11), (3.22) and (3.34), where we used (3.31) expression for $\sigma_e|_{n+1}$ in the first equation and (3.18) expression for $\Delta\varepsilon_v^p$ in the second equation. This system has to be solved for $(\Delta\bar{\varepsilon})$, $(\Delta\varepsilon_v^p)$ and (ΔE_{33}):

$$F_1 = \sigma_e|_{n+1} - \tilde{\sigma}_0\left(c_{n+1}^{(i)}, \bar{\varepsilon}_{n+1}^{(i)}\right) = \mu\frac{F\left(\Delta E_{33}\right) - 3\left(\Delta\bar{\varepsilon} + \frac{A_0}{\Delta_v}\Delta\varepsilon_v^p\right)}{1 + \frac{A_1}{\Delta_v}\frac{3\mu}{s_a^*}} - \tilde{\sigma}_0\left(c_{n+1}^{(i)}, \bar{\varepsilon}_{n+1}^{(i)}\right) \tag{3.35}$$

$$F_2 = \Delta\varepsilon_v^p - \Delta_v c_n^{(2)} A_f|_n a^{(2)}\Delta\bar{\varepsilon} \tag{3.36}$$

$$F_3 = \bar{s}_{33}^e + \frac{4}{3}\mu\Delta E_{33} + \left[1 + \frac{3\mu}{\sigma_e|_{n+1}}\left(\Delta\bar{\varepsilon} + \frac{A_{n+1}}{\Delta_v}\Delta\varepsilon_v^p\right)\right]\hat{p}_{33}|_{n+1} = 0 \tag{3.37}$$

where $F\left(\Delta E_{33}\right) = \sqrt{\frac{\bar{\sigma}_e^e}{\mu^2} + \frac{6\Delta E_{33}\bar{s}_{33}^e}{\mu} + 4(\Delta E_{33})^2}$ and equation (3.31) is used for the substitution of in the first equation.

Newton's method is used for the solution of the system. The first estimates for this method are given in (3.42).

3.2 First Estimates

We can acquire the initial values of $\Delta\bar{\varepsilon}$, $\Delta\varepsilon_v^p$ and ΔE_{33} in a similar way aw we did in the previous model. By differentiating the consistency condition, we already have the following expression (2.96) for $d\bar{\varepsilon}$:

$$d\bar{\varepsilon} = a_1 \mathbf{N} : d\mathbf{E}, \tag{3.38}$$

where $a_1 = \frac{2}{3D}$, $D = 1 + \frac{H}{3\mu} + \mu\left(\frac{A}{\Delta_v} + \frac{H_v}{3\mu}\right)$, and from (3.36) for $d\varepsilon_v^p$:

$$d\varepsilon_v^p = m d\bar{\varepsilon} = m a_1 \mathbf{N} : d\mathbf{E} \tag{3.39}$$

In this case, as only the $d\bar{\mathbf{E}}$ part of $d\mathbf{E}$ is known, we will create a system of equations with $d\bar{\mathbf{E}}$ on the right-hand side. In addition, as dE_{33} is unknown, we have a system of three equations with three unknowns.

As $d\mathbf{E} = d\bar{\mathbf{E}} + dE_{33}\mathbf{a}$, (3.38) equation is written as:

$$\begin{aligned} &\frac{3}{2}\left[1 + \frac{H}{3\mu} + \mu\left(\frac{A}{\Delta_v} + \frac{H_v}{3\mu}\right)\right] = \mathbf{N} : \left(d\bar{\mathbf{E}} + dE_{33}\mathbf{a}\right) \Rightarrow \\ &\frac{3}{2}\left[1 + \frac{H}{3\mu} + \mu\left(\frac{A}{\Delta_v} + \frac{H_v}{3\mu}\right)\right] - \mathbf{N} : \mathbf{a} \quad dE_{33} = \mathbf{N} : d\bar{\mathbf{E}} \end{aligned} \tag{3.40}$$

Next, we use the plane stress condition:

$$\dot{\sigma}_{33} = 0$$

together with equations (3.26) and (3.27):

$$\dot{\sigma}_{33} = 2\mu\left[\dot{e}_{33} - \left(\dot{\bar{\varepsilon}} + \frac{A}{\Delta_v}\dot{\varepsilon}_v^p\right) N_{33}\right] + \kappa\left(\dot{\varepsilon}_{kk} - \dot{\varepsilon}_v^p\right) = 0 \Rightarrow$$

$$2\mu\left[d\bar{\varepsilon}_{33} + dE_{33}a'_{33} - \left(d\bar{\varepsilon} + \frac{A}{\Delta_v}d\varepsilon_v^p\right) N_{33}\right] + \kappa\left(d\bar{E}_{kk} + dE_{33} - d\varepsilon_v^p\right) = 0 \Rightarrow$$

$$2\mu N_{33} d\bar{\varepsilon} + \left(2\mu\frac{A}{\Delta_v}N_{33} + \kappa\right) d\varepsilon_v^p - \left(\kappa + \frac{4}{3}\mu\right) dE_{33} = 2\mu\mathbf{a} : d\bar{\mathbf{e}} + \kappa d\bar{E}_{kk} \Rightarrow$$

$$\left[2\mu N_{33} + m\left(2\mu\frac{A}{\Delta_v}N_{33} + \kappa\right)\right] d\bar{\varepsilon} - \left(\kappa + \frac{4}{3}\mu\right) dE_{33} = (\kappa\boldsymbol{\delta} + 2\mu\mathbf{a}') : d\bar{\mathbf{E}} \tag{3.41}$$

Equations (3.40) and (3.41) are presented in matrix form as:

$$\begin{bmatrix} \frac{3}{2}\left[1 + \frac{H}{3G} + \mu\left(\frac{A}{\Delta_v} + \frac{H_v}{3G}\right)\right] & -\mu N_{33} \\ 2\mu N_{33} + m\left(2\mu\frac{A}{\Delta_v}N_{33} + \kappa\right) & -\left(\kappa + \frac{4}{3}\mu\right) \end{bmatrix} \begin{Bmatrix} d\bar{\varepsilon} \\ dE_{33} \end{Bmatrix} = \begin{Bmatrix} \mathbf{N} : d\bar{\mathbf{E}} \\ (\kappa\boldsymbol{\delta} + 2\mu\mathbf{a}') : d\bar{\mathbf{E}} \end{Bmatrix} \tag{3.42}$$

3.3 The Linearization moduli

In the previous chapter, in (2.99) equation, we have acquired the following expression for the linearization moduli:

$$\hat{\mathbf{C}} = (2\mu\boldsymbol{\mathcal{K}} + 3\kappa\boldsymbol{\mathcal{J}} - f_1\mathbf{NN} - f_2\boldsymbol{\delta}\mathbf{N})$$

where $f_1 = 2\mu a_1\left(1 + \frac{A}{\Delta_v}m\right)$ and $f_2 = \kappa m a_1$.

In plane strain problems, we can write the equation $d\sigma = \mathbf{C} : d\mathbf{E}$ in matrix form

$$\begin{Bmatrix} d\sigma_{11} \\ d\sigma_{22} \\ d\sigma_{33} \\ d\sigma_{12} \end{Bmatrix} = \begin{bmatrix} C_{11} & C_{12} & C_{13} & C_{14} \\ C_{21} & C_{22} & C_{23} & C_{24} \\ C_{31} & C_{32} & C_{33} & C_{34} \\ C_{41} & C_{42} & C_{43} & C_{44} \end{bmatrix} \begin{Bmatrix} dE_{11} \\ dE_{22} \\ dE_{33} \\ dE_{12} \end{Bmatrix}. \tag{3.43}$$

but in plane stress problems, the linearization moduli $\bar{\mathbf{C}}$ used in ABAQUS needs to be of the form:

$$\begin{Bmatrix} d\sigma_{11} \\ d\sigma_{22} \\ d\sigma_{12} \end{Bmatrix} = \begin{bmatrix} \bar{C}_{11} & \bar{C}_{12} & \bar{C}_{13} \\ \bar{C}_{21} & \bar{C}_{22} & \bar{C}_{23} \\ \bar{C}_{31} & \bar{C}_{32} & \bar{C}_{33} \end{bmatrix} \begin{Bmatrix} dE_{11} \\ dE_{22} \\ dE_{12} \end{Bmatrix}, \tag{3.44}$$

This form can be derived from equation (3.43) using the plane stress condition $d\sigma_{33} = 0$ or

$$\begin{aligned} d\sigma_{33} = C_{13}dE_{11} + C_{32}dE_{22} + C_{33}dE_{33} + 2C_{34}dE_{12} = 0 \Rightarrow \\ dE_{33} = -\frac{C_{13}dE_{11} + C_{32}dE_{22} + 2C_{34}dE_{12}}{C_{33}}, \end{aligned} \tag{3.45}$$

Thus, combining the last equation and equation (3.43) after some calculations we derive:

$$\begin{aligned} \bar{C}_{11} &= C_{11} - \frac{C_{13}}{C_{33}}C_{31}, \quad \bar{C}_{12} = C_{12} - \frac{C_{13}}{C_{33}}C_{32}, \quad \bar{C}_{13} = C_{14} - \frac{C_{13}}{C_{33}}C_{34}, \\ \bar{C}_{21} &= C_{21} - \frac{C_{23}}{C_{33}}C_{31}, \quad \bar{C}_{22} = C_{22} - \frac{C_{23}}{C_{33}}C_{32}, \quad \bar{C}_{23} = C_{24} - \frac{C_{23}}{C_{33}}C_{34}, \\ \bar{C}_{31} &= C_{41} - \frac{C_{43}}{C_{33}}C_{31}, \quad \bar{C}_{32} = C_{42} - \frac{C_{43}}{C_{33}}C_{32}, \quad \bar{C}_{33} = C_{44} - \frac{C_{43}}{C_{33}}C_{34}. \end{aligned}$$

For instance,

$$\begin{aligned} d\sigma_{11} &= C_{11}\,dE_{11} + C_{12}\,dE_{22} + C_{13}\,dE_{33} + 2C_{14}\,dE_{12} \\ &= C_{11}\,dE_{11} + C_{12}\,dE_{22} - \tfrac{C_{13}}{C_{33}}\left(C_{31}dE_{11} + C_{32}dE_{22} + 2C_{34}dE_{12}\right) + 2C_{14}\,dE_{12} \\ &= \left(C_{11} - \tfrac{C_{13}}{C_{33}}C_{31}\right)dE_{11} + \left(C_{12} - \tfrac{C_{13}}{C_{33}}C_{32}\right)\,dE_{22} + \left(C_{14} - \tfrac{C_{13}}{C_{33}}C_{34}\right)2\,dE_{12} \end{aligned} \tag{3.46}$$

Chapter 4

Forming Limit Diagrams

In this chapter the constitutive model developed for the three-phase TRIP steel is used to calculate "forming limit diagrams" for sheets of TRIP steels with a standard initial values of volume fractions of the phases. A forming limit diagram shows the maximum deformation which can be applied in a sheet, subjected in plane stress, until failure. We will assume that each sheet has an imperfection in the form of a narrow straight band with a reduced thickness. Across this band, the deformation gradient will be discontinuous, and, as a result, instabilities may be observed in this band which lead to failure. For comparison purposes, we will also calculate forming limit diagrams for a perfect sheet and sheets without the TRIP effect and we will compare those results.

4.1 Problem formulation

The discontinuities of the deformation gradient between the band and the other part of the sheet are expressed as:

$$F^b_{\alpha\beta} = F_{\alpha\beta} + \left[\frac{\partial u_\alpha}{\partial X_\beta}\right], \tag{4.1}$$

where $[\partial u_\alpha/\partial X_\beta]$ is the jump of the deformation gradient and $\mathbf{F}^b$ is the deformation gradient inside the band. The Greek letters α, β take values in range (1,2). The deformation gradient is constant in the direction parallel to the band and the jump appears in the vertical to the band direction, and, consequently, the jump is written in the following form:

$$\left[\frac{\partial u_\alpha}{\partial X_\beta}\right] = G_\alpha N_\beta, \tag{4.2}$$

where $\mathbf{N} = N_1\mathbf{e}_1 + N_2\mathbf{e}_2$ is the unit vector normal to the band, in the undeformed configuration and $\mathbf{G}$ is the jump in the normal derivative of $\mathbf{u}$. So, the deformation gradient inside the band is constant and has the form:

$$F^b_{\alpha\beta} = F_{\alpha\beta} + G_\alpha N_\beta. \tag{4.3}$$

So, for the determination of the deformation gradient inside the band we have to find $\mathbf{G}$.

The deformation gradient outside the band, in matrix form is:

$$[F_{ij}] = \begin{bmatrix} \lambda_1 & 0 & 0 \\ 0 & \lambda_2 & 0 \\ 0 & 0 & \lambda_3 \end{bmatrix} \tag{4.4}$$

and inside the band:

$$\left[F_{ij}^b\right] = \begin{bmatrix} \lambda_1 + G_1 N_1 & G_1 N_2 & 0 \\ G_2 N_1 & \lambda_2 + G_2 N_2 & 0 \\ 0 & 0 & \lambda_3^b \end{bmatrix} \tag{4.5}$$

where λ_1 and λ_2 are considered to be known.

In this part we use the 1^{st} Piola-Kirchhoff tensor, $\mathbf{t}$, for convenience. The 1^{st} Piola-Kirchhoff tensor can be related with the Cauchy stress tensor through the relation:

$$\mathbf{t} = J\mathbf{F}^{-1} \cdot \boldsymbol{\sigma}, \tag{4.6}$$

where $J = \det \mathbf{F}$. It can be proven that:

$$\dot{\mathbf{t}} = \mathbf{R} : \dot{\mathbf{F}}^T \tag{4.7}$$

where

$$R_{ijkl} = JF_{im}^{-1} F_{kn}^{-1} \left(L_{mjnl} + V_{mjnl}\right)$$

and

$$V_{ijkl} = \frac{1}{2}\left(\sigma_{ik}\delta_{jl} - \delta_{ik}\sigma_{jl} - \sigma_{il}\delta_{jk} - \delta_{il}\sigma_{jk}\right) + \sigma_{ij}\delta_{kl}.$$

Equation (4.7) is written as:

$$\dot{t}_{\alpha\beta} = R_{\alpha\beta lk}\dot{F}_{lk} = R_{\alpha\beta\gamma\delta}\dot{F}_{delta\gamma} + R_{\alpha\beta 33}\dot{F}_{33} \tag{4.8}$$

and

$$\dot{t}_{33} = R_{33kl}\dot{F}_{lk} = R_{33\delta\gamma} + R_{3333}\dot{F}_{33} \tag{4.9}$$

The Plane Stress condition implies that:

$$\dot{\sigma}_{33} = 0 \Rightarrow \dot{t}_{33} = R_{33\gamma\delta}\dot{F}_{\delta\gamma} + R_{3333}\dot{F}_{33} = 0 \Rightarrow$$

$$\dot{F}_{33} = -\frac{R_{33\gamma\delta}\dot{F}_{\delta\gamma}}{R_{3333}} \tag{4.10}$$

By substituting $\dot{F}_{33}$ in (4.8) equation, using the expression above, we have:

$$\dot{t}_{\alpha\beta} = R_{\alpha\beta\delta\gamma}\dot{F}_{\gamma\delta} + R_{\alpha\beta 33}\left(-\frac{R_{33\gamma\delta}\dot{F}_{\delta\gamma}}{R_{3333}}\right) = \left(R_{\alpha\beta\delta\gamma}\dot{F}_{\gamma\delta} - R_{\alpha\beta 33}\frac{R_{33\gamma\delta}}{R_{3333}}\right)\dot{F}_{\delta\gamma}. \tag{4.11}$$

So, the constitutive equation which we will use for this analysis has the form:

$$\dot{t}_{\alpha\beta} = C_{\alpha\beta\gamma\delta}\dot{F}_{\delta\gamma}, \tag{4.12}$$

where $C_{\alpha\beta\gamma\delta} = \left(R_{\alpha\beta\gamma\delta} - R_{\alpha\beta33}\frac{R_{33\gamma\delta}}{R_{3333}}\right)$.

In a similar way, we can derive the constitutive equation inside the band:

$$\dot{t}^b_{\alpha\beta} = C^b_{\alpha\beta\gamma\delta}\dot{F}^b_{\gamma\delta}, \tag{4.13}$$

where $C^b_{\alpha\beta\gamma\delta} = \left(R^b_{\alpha\beta\gamma\delta} - R^b_{\alpha\beta33}\frac{R^b_{33\gamma\delta}}{R^b_{3333}}\right)$.

The equilibrium across the band indicates that:

$$T_\alpha = T^b_\alpha \Rightarrow$$
$$HN_\beta t_{\beta\alpha} = H^b N_\beta t^b_{\beta\alpha}. \tag{4.14}$$

the rate form of which is:

$$H\dot{N}_\beta t_{\beta\alpha} = H^b \dot{N}_\beta t^b_{\beta\alpha}. \tag{4.15}$$

Now, combining equations (4.12), (4.13) and (4.18) we find:

$$\mathbf{A}\cdot\dot{\mathbf{G}} = \mathbf{B}\cdot\dot{\mathbf{b}} \tag{4.16}$$

where $A_{\alpha\beta} = N_\gamma C^b_{\gamma\alpha\delta\beta}N_\gamma$, $B_{\alpha\beta} = N_\gamma\left(\frac{H}{H_b}C_{\gamma\alpha\beta\beta} - C^b_{\gamma\alpha\beta\beta}\right)$ and $b_\alpha = \lambda_\alpha$.

In the case of a perfect sheet, or $H = H^b$, $\mathbf{C} = \mathbf{C}^b$. As a result, it is obvious from (4.16), $B_{\alpha\beta} = 0$ and $\dot{G}_{\alpha\beta} = 0$. Therefore, along a perfect sheet the deformation is homogenous, or $\mathbf{F} = \mathbf{F}^b$. The local necking bifurcation condition is met when $\det[\mathbf{A}] = 0$.

In a sheet with a straight narrow band of thickness $H^b < H$, $\mathbf{B}$ does not vanish, so equation (4.16) can be solved for $\dot{\mathbf{G}}$. The localization condition is met when $d|\mathbf{G}|/\,d\lambda_1 = \infty$, or when $\det[\mathbf{A}] = 0$.

For given ΔF in plane $X_1 - X_2$ we can compute ΔG and ΔF^b using equation (4.16). Thus, we will use the equilibrium across the band itself, in order to get a higher accuracy. The equilibrium suggests that:

$$\mathbf{T}_{n+1} = \mathbf{T}^b_{n+1} \tag{4.17}$$

If we set:

$$\mathbf{T}_{n+1} = \mathbf{T}_n + \dot{\mathbf{T}}_n\Delta t$$

and

$$\mathbf{T}^b_{n+1} = \mathbf{T}^b_n + \dot{\mathbf{T}}^b_n\Delta t$$

we derive:

$$A_{\alpha\beta}|_n\Delta G_\beta = B_{\alpha\beta}b_\alpha|_n\Delta t + \frac{1}{H^b}\left(T_\alpha|_n - T^b_\alpha|_n\right) \tag{4.18}$$

In this analysis the tensor of the logarithmic strains out of the band has the form:

$$\mathbf{E} = \begin{bmatrix} E_{11} & 0 & 0 \\ 0 & E_{22} & 0 \\ 0 & 0 & E_{33} \end{bmatrix} \tag{4.19}$$

where E_{11} and E_{22} are considered known, as well as, λ_1 and λ_2 while λ_{33} will be calculated using the plane stress condition. As we have mentioned previously, in this analysis, the rates of change of the strains E_1 and E_2 must be proportional to each other:

$$\frac{dE_2}{dE_1} = \rho \Rightarrow$$
$$\frac{E_1}{E_2} = \rho \tag{4.20}$$

where ρ is constant during an analysis.

Last equation implies:

$$\lambda_2 = \lambda_1^{\rho} \tag{4.21}$$

Every set of calculations is carried out for a certain value ρ and H_b/H . At the start of each increment we have a standard $\Delta\lambda_1$, so we define the following quantities at the end of the increment:

$$\lambda_1|_{n+1} = \lambda_1|_n + \Delta\lambda_1 \tag{4.22}$$

$$\lambda_2|_{n+1} = (\lambda_1|_{n+1})^{\rho} \tag{4.23}$$

So, at the start of each increment we assume that the values of $\boldsymbol{\sigma}_n$, $\mathbf{F}_n$, $\varepsilon_v^p|_n$, $\bar{\varepsilon}_n$, $\bar{\varepsilon}_n^{(i)}$, $c_n^{(i)}$ and $\bar{\mathbf{F}}_{n+1}$ are known, where $\bar{\mathbf{F}}_{n+1}$ is defined as :

$$[\bar{F}_{ij}] = \begin{bmatrix} \lambda_1|_{n+1} & 0 & 0 \\ 0 & (\lambda_1|_{n+1})^{\rho} & 0 \\ 0 & 0 & 0 \end{bmatrix} = known \tag{4.24}$$

Then, we determine the uniform solution outside the band by using the plane stress algorithm presented in the previous chapter. Next, we calculate $\Delta\mathbf{G}$ and subsequently $\mathbf{F}_b$ and finally, we determine the uniform solution inside the band using the same plane stress algorithm. In each increment, λ_1 is increased by a small quantity $\Delta\lambda_1$, until the instability condition $\det \mathbf{A}$ is met. So, we will acquire the minimum value of E_{11} until failure, for a certain value of Ψ.

4.2 Results

The initial volume fractions of the three phases in the TRIP steel are assumed to be $c_1 = 0.84$ for ferrite, $c_2 = 0.072$ for austenite and $c_3 = 0.88$ for martensite. The hardening curve of each phase has the following form:

$$\sigma_y^{(i)} = A^{(i)}\left(1 + \frac{\bar{\varepsilon}^{(i)}}{b^{(i)}}\right)^{\frac{1}{\eta^{(i)}}}$$

The values of $A^{(i)}, b^{(i)}, \eta^{(i)}$ determine the form of the hardening curve. $A^{(i)}$ is measured in MPa, while $b^{(i)}$ and $\eta^{(i)}$ are dimensionless quantities. The hardening curves of ferrite and martensite were acquired from experimental data from the Technical steel research [21]. In

particular, for the ferritic phase we used the data of the annealed ferritic steel DOCOL 600 and for the martensitic phase we used the data of the partly martensitic steel DOCOL 1400 (volume fraction of martensite 95%). Regarding the retained austenite, we used the hardening curved used by Papadioti [12]. The values of the constants for each phase are presented in tables 4.1, 4.2 and 4.3:

Table 4.1: Hardening parameters of ferrite

$A^{(1)}$	$260(MPa)$
$b^{(1)}$	0.0042
$\eta^{(1)}$	4.25

Table 4.2: Hardening parameters of austenite

$A^{(2)}$	$550(MPa)$
$b^{(2)}$	0.01
$\eta^{(2)}$	4.2

Table 4.3: Hardening parameters of martensite

$A^{(3)}$	$1132(MPa)$
$b^{(3)}$	0.0042893
$\eta^{(3)}$	16.6567

In the calculations we use the values $E = 210$ GPa and $v = 0.3$ for the elastic Young's modulus and Poisson's ratio and the relative volume change associated with the martensitic transformation is taken to be $\Delta v = 0.02$. The values of the parameters that enter the transformation kinetics model are shown in Table 4.4.

We set $\mathbf{N} = \cos\Psi\mathbf{e}_1 + \sin\Psi\mathbf{e}_2$, where Ψ is the angle of inclination of the band relative to the X_1 axis in the undeformed configuration, and for every value of $\rho = dE_{11}/dE_{22}$, we carry out calculations to determine the minimum localization strain by scanning the range $0^o < \Psi < 90^o$. So, each point in the diagram corresponds to a certain value of $\rho = dE_{11}/dE_{22}$. The coordinate E_{11}^{crit} of this point in the diagram represents the minimum deformation until failure, of all possible orientations of the imperfection (for a standard ρ). The other coordinate is $E_{22}^{crit} = \rho E_{11}^{crit}$. The value of Ψ where E_{11}^{crit} is minimum is Ψ_{crit} for a certain ρ. For every different value of ρ we acquire a different point.
Figure 4.1 illustrates forming limit curves obtained for imposed proportional straining ρ for two different values of the initial thickness imperfection, namely $H_b/H = 0.999$ and $H_b/H = 0.99$ and for the case without imperfection i.e. $H_b/H = 1$. The three solid curves correspond to the TRIP steel, whereas the dashed curves are for the non-transforming steel. As we can see, the TRIP effect increases the necking localization strains. This result was also presented by Papatriantafillou et al. [14] and Papadioti [12], who developed constitutive models for four-phase TRIP steels.
Figure 4.2 shows the values of Ψ_{crit} for different values of ρ.

Table 4.4: Costants of the kinetic model used in the calculations

E	$210(GPa)$
v	0.3
N_{phases}	3
A_0	0.012
A_1	0.057
s_a^*	$496(MPa)$
Δ_v	0.02
v_p	$4.18 \times 10^{-18} \quad (m^3)$
k	46
m	3.45
N	$2 \times 10^{19} \quad (m^{-3})$
a_ε	0.03
E_{str}	$500 \quad (J/mol)$
γ_s	$0.15 \quad (J/m^2)$
ρ	3×10^{-5}
T	$283.15K = 10^oC$
X_{Mn}	1.5898×10^{-2}
X_C	3.61326×10^{-2}

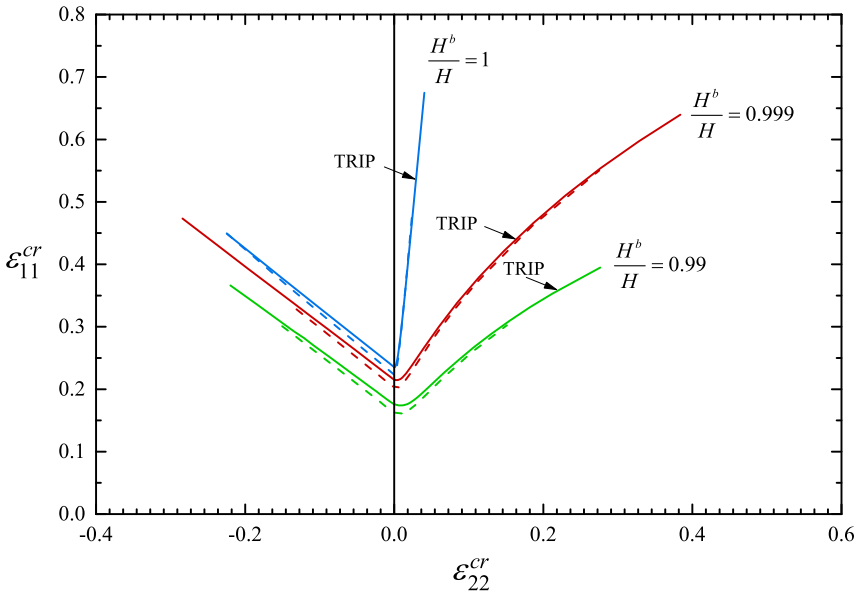

Figure 4.1: Forming limit curves for two different values of initial thickness inhomogeneities $H_b/H = 0.999$ and $H_b/H = 0.99$. The solid lines correspond to the TRIP steel, whereas the dashed lines are for a non-transforming steel.

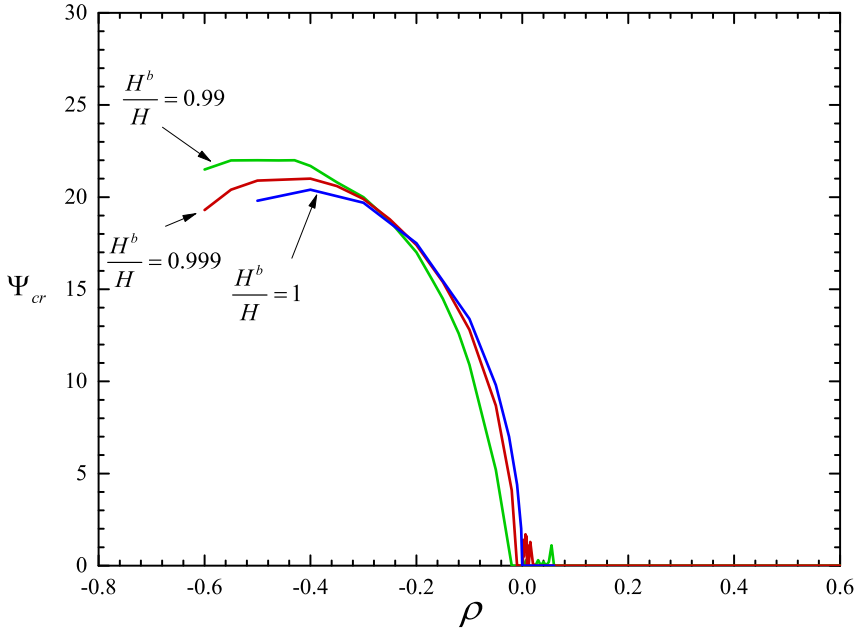

Figure 4.2: Ψ_{crit} with respect to ρ for sheets made of TRIP steels

Chapter 5

Closure

5.1 Comments on the results and conclusions

We use homogenisation theory to develop a constitutive model for TRIP steels. In particular, we consider three-phase TRIP steels that consist of a ferritic matrix with dispersed austenite, which transforms gradually into martensite as the material deforms plastically. The total strain can be split into elastic, plastic, and transformation parts. Standard isotropic linear hypoelasticity of homogeneous solids is used in order to describe the elastic behavior of the TRIP steels since the elastic properties of all phases are fundamentally the same. The homogenization techniques for non-linear composites are used to determine the effective properties and overall behavior of TRIP steels. The transformation part is proportional to the rate of change of the volume fraction of martensite due to martensitic transformation, which is described by the transformation kinetics model proposed by Haidemenopoulos, Aravas, Bellas [5].
A method for the numerical integration of the resulting constitutive equations in the context of a displacement driven finite element formulation was developed and the model was implemented into the ABAQUS. We also developed a method for the numerical integration of the constitutive model under plane stress conditions.
In the final part, we used the plane stress model for the calculation of the forming limit diagrams of a three-phase low-alloy TRIP steel with certain initial volume fractions of the phases. The form of the diagrams shows that the TRIP effect has a serious impact on the results, and thus, it has to be considered. Also, the results are consistent with those in the works of Papadioti[12] and Papatriantafillou[14].

5.2 Suggestions for future research

It is known that materials which can afford a high plastic deformation until failure are more resistant to cracking. As we have already seen, TRIP steels have this property, so they can be used in applications where fracture resistance is required. As a result, we could propose the development of a constitutive model for the cyclic response of composite materials, using a more sophisticated homogenisation method.

Finally, in chapter 4 we derived the hardening curves of the constituent phases from a detailed bibliographic search. So in order to further improve the simulation of the mechanical behavior of TRIP steels, we could develop an experimental method in order to measure the hardening of the constituent phases. This way we would have more precise data.

Chapter 6

Appendices

6.1 Details of the calculations

The Jacobian matrix of the system of equations (3.35), (3.36) and (3.37):

$$F_1 = \sigma_e|_{n+1} - \tilde{\sigma}_0\left(c_{n+1}^{(i)}, \bar{\varepsilon}_{n+1}^{(i)}\right) = \mu\frac{F\left(\Delta E_{33}\right) - 3\left(\Delta\bar{\varepsilon} + \frac{A_0}{\Delta_v}\Delta\varepsilon_v^p\right)}{1 + \frac{A_1}{\Delta_v}\frac{3\mu}{s_a^*}} - \tilde{\sigma}_0\left(c_{n+1}^{(i)}, \bar{\varepsilon}_{n+1}^{(i)}\right) \tag{6.1}$$

$$F_2 = \Delta\varepsilon_v^p - \Delta_v c_n^{(2)} A_f|_n a^{(2)}\Delta\bar{\varepsilon} \tag{6.2}$$

$$F_3 = \bar{s}_{33}^e + \frac{4}{3}\mu\Delta E_{33} + \left[1 + \frac{3\mu}{\sigma_e|_{n+1}}\left(\Delta\bar{\varepsilon} + \frac{A_{n+1}}{\Delta_v}\Delta\varepsilon_v^p\right)\right]\hat{p}_{n+1} = 0 \tag{6.3}$$

where $F\left(\Delta E_{33}\right) = \sqrt{\frac{\bar{\sigma}_e^e}{\mu^2} + \frac{6\Delta E_{33}\bar{s}_{33}^e}{\mu} + 4(\Delta E_{33})^2}$,

$$J_{11} = \frac{\partial F_1\left(\Delta\bar{\varepsilon}, \Delta\varepsilon_v^p, \Delta E_{33}\right)}{\partial\Delta\bar{\varepsilon}} = \frac{\partial\sigma_e|_{n+1}}{\partial\Delta\bar{\varepsilon}} - \frac{\partial\tilde{\sigma}_0}{\partial\Delta\bar{\varepsilon}} =$$

$$= \frac{\partial\sigma_e|_{n+1}}{\partial\Delta\bar{\varepsilon}} - \sum_{i=1}^{3}\frac{\partial\tilde{\sigma}_0}{\partial\sigma_0^{(i)}}\frac{\partial\sigma_0^{(i)}}{\partial\bar{\varepsilon}^{(i)}}\frac{\partial\bar{\varepsilon}^{(i)}}{\partial\bar{\varepsilon}} = \frac{\partial\sigma_e|_{n+1}}{\partial\Delta\bar{\varepsilon}} - \sum_{i=1}^{3}\frac{\partial\tilde{\sigma}_0}{\partial\sigma_0^{(i)}}h^{(i)}a_n^{(i)},$$

$$J_{12} = \frac{\partial F_1\left(\Delta\bar{\varepsilon}, \Delta\varepsilon_v^p, \Delta E_{33}\right)}{\partial\Delta\varepsilon_v^p} = \frac{\partial\sigma_e|_{n+1}}{\partial\Delta\varepsilon_v^p} - \frac{\partial\tilde{\sigma}_0}{\partial\Delta\varepsilon_v^p} = \frac{\partial\sigma_e|_{n+1}}{\partial\varepsilon_v^p} - \sum_{i=1}^{3}\frac{\partial\tilde{\sigma}_0}{\partial c^{(i)}}\frac{\partial c^{(i)}}{\partial\Delta\varepsilon_v^p},$$

$$J_{13} = \frac{\partial F_1\left(\Delta\bar{\varepsilon}, \Delta\varepsilon_v^p, \Delta E_{33}\right)}{\partial\Delta E_{33}} = \frac{\partial\sigma_e|_{n+1}}{\partial\Delta E_{33}},$$

$$J_{21} = \frac{\partial F_2\left(\Delta\bar{\varepsilon}, \Delta\varepsilon_v^p, \Delta E_{33}\right)}{\partial\Delta\bar{\varepsilon}} = -\Delta_v c_n^{(2)} A_f|_n a_n^{(2)},$$

$$J_{22} = \frac{\partial F_2\left(\Delta\bar{\varepsilon}, \Delta\varepsilon_v^p, \Delta E_{33}\right)}{\partial\Delta\varepsilon_v^p} = 1,$$

$$J_{23} = \frac{\partial F_2\left(\Delta\bar{\varepsilon}, \Delta\varepsilon_v^p, \Delta E_{33}\right)}{\partial\Delta E_{33}} = 0,$$

$$J_{31}=\frac{\partial F_3\left(\Delta\bar{\varepsilon},\Delta\varepsilon_v^p,\Delta E_{33}\right)}{\partial\Delta\bar{\varepsilon}}=\frac{\partial F_3}{\Delta\bar{\varepsilon}}+\frac{\partial F_3}{\partial\sigma_e|_{n+1}}\frac{\partial\sigma_e|_{n+1}}{\partial\Delta\bar{\varepsilon}}+\frac{\partial F_3}{\partial\hat{p}_{n+1}}\frac{\partial\hat{p}_{n+1}}{\Delta\bar{\varepsilon}}=3\mu\frac{\hat{p}_{n+1}}{\sigma_e|_{n+1}}+\frac{\partial F_3}{\partial\sigma_e|_{n+1}}\frac{\partial\sigma_e|_{n+1}}{\partial\Delta\bar{\varepsilon}},$$

$$J_{32}=\frac{\partial F_3\left(\Delta\bar{\varepsilon},\Delta\varepsilon_v^p,\Delta E_{33}\right)}{\partial\Delta\varepsilon_v^p}=\frac{\partial F_3}{\partial\Delta\varepsilon_v^p}+\frac{\partial F_3}{\partial\sigma_e|_{n+1}}\frac{\partial\sigma_e|_{n+1}}{\partial\Delta\varepsilon_v^p}+\frac{\partial F_3}{\partial\hat{p}_{n+1}}\frac{\partial\hat{p}_{n+1}}{\partial\Delta\varepsilon_v^p}=$$

$$=\frac{3\mu}{\sigma_e|_{n+1}}\frac{A_{n+1}}{\Delta_v}\hat{p}_{n+1}+\frac{\partial F_3}{\partial\sigma_e|_{n+1}}\frac{\partial\sigma_e|_{n+1}}{\partial\Delta\varepsilon_v^p}+\frac{\partial F_3}{\partial\hat{p}_{n+1}}\frac{\partial\hat{p}_{n+1}}{\partial\Delta\varepsilon_v^p},$$

$$J_{33}=\frac{\partial F_3\left(\Delta\bar{\varepsilon},\Delta\varepsilon_v^p,\Delta E_{33}\right)}{\partial\Delta E_{33}}=\frac{\partial F_3}{\partial\Delta E_{33}}+\frac{\partial F_3}{\partial\sigma_e|_{n+1}}\frac{\partial\sigma_e|_{n+1}}{\partial\Delta E_{33}}+\frac{\partial F_3}{\partial\hat{p}_{n+1}}\frac{\partial\hat{p}_{n+1}}{\partial\Delta E_{33}}=$$

$$=\frac{4}{3}\mu+\frac{\partial F_3}{\partial\sigma_e|_{n+1}}\frac{\partial\sigma_e|_{n+1}}{\partial\Delta E_{33}}+\frac{\partial F_3}{\partial\hat{p}_{n+1}}\frac{\partial\hat{p}_{n+1}}{\partial\Delta E_{33}}$$

.

The derivatives appeared in the calculations of the Jacobian are:
$\frac{\partial c_{n+1}^{(1)}}{\partial\Delta\varepsilon_v^p}=-c_{n+1}^{(1)},\ \frac{\partial c_{n+1}^{(3)}}{\partial\Delta\varepsilon_v^p}=\frac{1}{\Delta_v},$
$\frac{\partial c_{n+1}^{(2)}}{\partial\Delta\varepsilon_v^p}=-\left(\frac{\partial c_{n+1}^{(1)}}{\Delta\varepsilon_v^p}+\frac{\partial c_{n+1}^{(3)}}{\partial\Delta\varepsilon_v^p}\right)=c_{n+1}^{(1)}-\frac{1}{\Delta_v},$
$\frac{\partial\sigma_e|_{n+1}}{\partial\Delta\bar{\varepsilon}}=\frac{-3\mu}{1+\frac{3\mu}{s_a^*}\frac{A_1}{\Delta_v}\Delta\varepsilon_v^p},$
$\frac{\partial\sigma_e|_{n+1}}{\partial\varepsilon_v^p}=\frac{-3\mu}{\Delta_v+\frac{3\mu}{s_a^*}A_1\Delta\varepsilon_v^p}\left(A_0+A_1\frac{\sigma_e|_{n+1}}{s_a^*}\right),$
$\frac{\partial\sigma_e|_{n+1}}{\partial\Delta E_{33}}=\frac{\mu}{1+\frac{3\mu}{s_a^*}\frac{A_1}{\Delta_v}\Delta\varepsilon_v^p}\frac{\partial F\left(\Delta E_{33}\right)}{\partial\Delta E_{33}},$
$\frac{\partial F_3}{\partial\sigma_3|_{n+1}}=\frac{-3\mu}{\sigma_e|_{n+1}}\left(\Delta\bar{\varepsilon}+\frac{A_0}{\Delta_v}\right)\frac{\hat{p}_{n+1}}{\sigma_e|_{n+1}},$
$\frac{\partial F_3}{\partial\hat{p}_{n+1}}=1+3\mu\left(\frac{\Delta\bar{\varepsilon}}{\sigma_e|_{n+1}}\left(\frac{A_0}{\sigma_3|_{n+1}}+\frac{A_1}{s_a^*}\right)\frac{\Delta\varepsilon_v^p}{\Delta_v}\right),$
$\frac{\partial F\left(\Delta E_{33}\right)}{\partial\Delta E_{33}}=\frac{1}{F}\left(3\frac{\bar{s}_{33}^e}{\mu}+4\Delta E_{33}\right),$
$\frac{\partial\hat{p}_{n+1}}{\partial\Delta\varepsilon_v^p}=-\kappa,\ \frac{\partial\hat{p}_{n+1}}{\partial\Delta E_{33}}=\kappa\ .$
Also, the following quantities
$\left.\frac{\partial\tilde{\sigma}_0}{\partial\sigma_0^{(i)}}\right|_{n+1},\left.\frac{\partial\tilde{\sigma}_0}{\partial c^{(i)}}\right|_{n+1}=known$, for $i=1,2,3,$
can been acquired by the solution of the optimization problem, while
$h^{(i)}=\frac{\partial\sigma_0^{(i)}}{\partial\bar{\varepsilon}^{(i)}}$, for $i=1,2,3,$
are known form the hardening curves of each phase.

Bibliography

[1] Analysis User's Manual, Version 6.11, © Dassault Systemes (2011).

[2] N. Aravas and P. Ponte Castañeda, 'Numerical methods for porous metals with deformation-induced anisotropy', *Comp. Methods Appl. Mech. Eng. 193* (2004).

[3] K. Danas, P. Ponte Castañeda, 'A finite-strain model for viscoplastic anisotropic porous media: I – Theory', *Eur. J. Mechanics A/Solids 28* (2009a).

[4] K. Danas, P. Ponte Castañeda, 'A finite-strain model for viscoplastic anisotropic porous media: II – Applications', *Eur. J. Mechanics A/Solids 28* (2009b).

[5] G. N. Haidemenopoulos, N. Aravas, I. Bellas, 'Kinetics of strain inducted transformation of dispersed austenite in low alloy TRIP steels', *Materials Science and Engineering A* (2014).

[6] M. Kailasam and P. Ponte Castañeda, 'A general constitutive theory for linear and nonlinear particulate media with microstructure evolution', *J. Mech. Phys. Solids 46* (1998).

[7] G. B. Olson and M. Cohen, 'Kinetics of strain-induced martensitic nucleation', *Metall. Trans. 6A* (1975).

[8] G. B. Olson and M. Cohen, 'A general mechanism of martensitic nucleation: Part I. General con-cepts and the FCC-HCP transformation', *Metall. Trans. 7A* (1976).

[9] G. B. Olson and M. Cohen, 'A general mechanism of martensitic nucleation: Part II. FCC-BCC and other martensitic transformations', *Metall. Trans. 7A* (1976).

[10] G. B. Olson and M. Cohen, 'A general mechanism of martensitic nucleation: Part III. Kinetics of martensitic nucleation', *Metall. Trans. 7A* (1976).

[11] I. Papadioti, K. Danas, N. Aravas 'A methodology for the estimation of the effective yield function of isotropic composites', *International Journal of Solids and Structures* (2016).

[12] I. Papadioti, 'Non linear Homogenization methods with applications to TRIP steels', *PhD Thesis, University of Thessaly* (2016).

[13] I. Papatriantafillou, 'TRIP steels: Constitutive modeling and computational issues', PhD thesis, University of Thessaly (2005).

[14] I. Papatriantafillou, M. Agoras, N. Aravas and G. Haidemenopoulos, 'Constitutive modeling and finite element methods for TRIP steels', *Comp. Methods Appl. Mech. Eng. 195* (2006).

[15] P. Ponte Castañeda, 'The effective mechanical properties of nonlinear isotropic composites', *J. Mech. Phys. Solids 39* (1991).

[16] P. Ponte Castañeda, 'New variational principles in plasticity and their application to composite materials', *J. Mech. Phys. Solids 40* (1992).

[17] P. Ponte Castañeda, 'Nonlinear composite materials: Effective constitutive behavior and mi-crostructure evolution', in Continuum Micromechanics, CISM Courses and Lectures No. 377 (ed. P. Suquet), Springer-Verlag (1997).

[18] P. Ponte Castañeda, 'Nonlinear composites', *Advances in Applied Mechanics 34* (1998).

[19] R. G. Stringfellow, D. M. Parks and G. B. Olson, 'A constitutive model for transformation plasticity accompanying strain-induced martensitic transfrmation in metastable austenitic steels' *Acta metall. mater. 40* (1992).

[20] P. Suquet, 'Overall properties of nonlinear composites: a modefied secan moduli theory and its link with Ponte Castañeda's nonlinear variational procedure' *CR Acad Sci Paris II 320* (1995).

[21] Technical Steel Research: 'Modeling of mechanical properties and local deformation of high-strength multi-phase steels', Final Report, European Commission, Contract No. 7210-Pr/044, (2002).

[22] M. Zaidman, P. Ponte Castañeda, 'The finite deformation of nonlinear composite Materials–II. Evolution of the microstructure' *Int. J. Solids Struct. 33* (1996).